

We are IntechOpen, the world's leading publisher of Open Access books Built by scientists, for scientists

6,900

Open access books available

186,000

International authors and editors

200M

Downloads

Our authors are among the

154

Countries delivered to

TOP 1%

most cited scientists

12.2%

Contributors from top 500 universities



WEB OF SCIENCE™

Selection of our books indexed in the Book Citation Index
in Web of Science™ Core Collection (BKCI)

Interested in publishing with us?
Contact book.department@intechopen.com

Numbers displayed above are based on latest data collected.
For more information visit www.intechopen.com



Nonlinear Unknown-Input Observer-Based Systems for Secure Communication

Robert N.K. Loh and Manohar K. Das

Additional information is available at the end of the chapter

<http://dx.doi.org/10.5772/intechopen.69239>

Abstract

Secure communication employing chaotic systems is considered in this chapter. Chaos-based communication uses chaotic systems as its backbone for information transmission and extraction, and is a field of active research and development and rapid advances in the literature. The theory and methods of synchronizing chaotic systems employing unknown input observers (UIOs) are investigated. New and novel results are presented. The techniques developed can be applied to a wide class of chaotic systems. Applications to the estimation of a variety of information signals, such as speech signal, electrocardiogram, stock price data hidden in chaotic system dynamics, are presented.

Keywords: chaotic secure communication, underwater acoustic communication, chaos, unknown input observers, nonlinear observers, reduced-order observers

1. Introduction

With the advances in computing and communication technologies, among others, underwater acoustic communication (UAC) techniques [1–6] have emerged as the predominant mode of underwater communication because of its one key advantage over conventional electromagnetic communication, namely, relatively low attenuation of acoustic waves in water. However, their performance is severely affected by a number of factors, including limited channel bandwidth, time-varying channel characteristics, complex ambient noise, and multipath distortion that results from multiple reflections of sound waves from top and bottom surfaces of water, especially in a relatively shallow waterbody.

Over the past decade, chaos-based underwater acoustic communication (CUAC) techniques have attracted a lot of interest from a number of researchers [7–12], because such techniques are potentially more cost-effective (for example, requiring lesser number of component modules) compared with conventional communication schemes. The CUAC techniques proposed to date can be broadly divided into two categories, namely, coherent detection based CUAC methods [7], and non-coherent detection based CUAC techniques. The coherent detection based methods rely on synchronization to reconstruct a copy of the transmitted signal at the receiver end, whereas non-coherent detection methods [8–12] utilize a variety of data recovery methods without requiring any synchronized reconstruction of the transmitted message.

In this chapter, we focus our attention on the synchronization based CUAC techniques, especially on observer-based synchronization methods, because the underlying theory is very well understood and has proven to be reliable and robust in many control applications. Also, such methods may potentially turn out to be easier to implement, as compared with many non-coherent CUAC techniques.

At the outset, we should point out that the main goal of this chapter is to present the fundamental concepts of observer-based chaotic synchronization and their applications to secure chaotic communication. With this in mind and owing to space limitation, we omit discussion of the robustness issues [13–23] of such techniques here. However, we should point out that the theory of robust observer design in the presence of noise and uncertainties has been well researched in control literature, and these ideas are deemed to be useful for synchronized based CUAC as well [18–23].

The methodologies used for CUAC have many things in common with chaos-based wired and wireless communication. Research and development in these fields have been advancing rapidly in the literature [7–16]. In contrast to conventional communication systems which use sinusoidal carriers to transmit information, chaos-based communication uses chaotic systems as its backbone for information transmission and recovery. The advantages of employing chaos-based systems include, among others, (i) the communication is difficult to detect and decrypt; (ii) the transmission is hidden from unauthorized receivers; (iii) the communication is more resistant to jamming and interferences because of the broadband characteristics of the chaos-based carriers. The advantages above are due to the following characteristics: (i) a chaotic system is dissipative; (ii) chaotic systems have unstable equilibrium points; (iii) its trajectories are aperiodic and bounded; and (iv) its trajectories have a sensitive dependence on their initial conditions, i.e., trajectories originated from slightly different initial conditions will soon become totally different. We remark that some of these characteristics may, in fact, be undesirable.

The organization of this chapter is as follows. Section 2 introduces three nonlinear chaotic systems that are utilized for designing chaotic communication systems in follow-up sections. Next a general discussion of unknown input observers is presented in Section 3. Section 4 presents the theory and design of unknown input observers for chaotic secure communication. Finally, the conclusions and plan for future research are provided in Section 5.

2. Nonlinear systems with application in chaotic communication

Consider a general nonlinear system described by

$$\begin{cases} \dot{\mathbf{x}} = \mathbf{f}(\mathbf{x}, \mathbf{d}) \\ \mathbf{y} = \mathbf{h}(\mathbf{x}, \mathbf{d}), \end{cases} \quad (1)$$

where $\mathbf{x} \in \mathbb{R}^n$ is the system state vector, $\mathbf{y} \in \mathbb{R}^m$ the output measurement, $\mathbf{d} \in \mathbb{R}^r$ an unknown disturbance vector which can be treated as a message vector that carries useful information; $\mathbf{f} : \mathbb{R}^n \times \mathbb{R}^r \rightarrow \mathbb{R}^n$ is a smooth vector field, $\mathbf{h} : \mathbb{R}^n \times \mathbb{R}^r \rightarrow \mathbb{R}^m$ a smooth function, $\mathbf{f}(\mathbf{0}, \mathbf{0}) = \mathbf{0}$ and $\mathbf{h}(\mathbf{0}, \mathbf{0}) = \mathbf{0}$.

The unknown disturbance \mathbf{d} in (1) is assumed to be generated by the exosystem

$$\begin{cases} \mathbf{d} = \mathbf{M}\mathbf{m}, \\ \dot{\mathbf{m}} = \mathbf{f}_m(\mathbf{m}, \mathbf{x}), \end{cases} \quad (2)$$

where $\mathbf{m} \in \mathbb{R}^r$ is the message state, $\mathbf{M} \in \mathbb{R}^{r \times r}$ is a “picking matrix” that picks the appropriate components m_i of \mathbf{m} to form \mathbf{d} , $\mathbf{f}_m : \mathbb{R}^r \times \mathbb{R}^n \rightarrow \mathbb{R}^r$ is a smooth vector field, and $\mathbf{f}_m(\mathbf{0}, \mathbf{0}) = \mathbf{0}$.

Eqs. (1) and (2) is widely used for the design of linear and nonlinear observers, unknown input observers (UIO), and unknown input observers for secure communication [24–46]. When applied to the design of unknown input observers (UIOs) for secure communication based on chaotic systems, (1) and (2) can be combined and expressed as

$$\begin{cases} \dot{\mathbf{x}} = \mathbf{f}(\mathbf{x}, \mathbf{m}) = \mathbf{f}(\mathbf{x}) + \mathbf{B}_m(\mathbf{x})\mathbf{M}\mathbf{m} = \mathbf{A}\mathbf{x} + \mathbf{g}(\mathbf{x}) + \mathbf{B}_m(\mathbf{x})\mathbf{M}\mathbf{m}, \\ \dot{\mathbf{m}} = \mathbf{f}_m(\mathbf{m}, \mathbf{x}) = \mathbf{A}_m\mathbf{m} + \mathbf{\Psi}\mathbf{x}, \\ \mathbf{y} = \mathbf{h}(\mathbf{x}, \mathbf{m}), \quad (\mathbf{d} = \mathbf{M}\mathbf{m}), \end{cases} \quad (3)$$

where $\mathbf{A}\mathbf{x}$ is the linear part of $\mathbf{f}(\mathbf{x})$, $\mathbf{g}(\mathbf{x}) \in \mathbb{R}^{n \times 1}$ and $\mathbf{B}_m(\mathbf{x}) \in \mathbb{R}^{n \times r}$, while \mathbf{m} ($\mathbf{d} = \mathbf{M}\mathbf{m}$) is now treated as the message signal, and $\mathbf{f}_m(\mathbf{m}, \mathbf{x}) = \mathbf{A}_m\mathbf{m} + \mathbf{\Psi}\mathbf{x}$, where $\mathbf{A}_m \in \mathbb{R}^{r \times r}$ is a constant matrix. The linear model in the second equation is commonly used in the literature, see for example [25]. In many applications, the message model can be simplified by setting $\mathbf{A}_m = \mathbf{0}$ and $\mathbf{\Psi} = \mathbf{0}$. Further, (3) may become a system with *state-dependent* or *multiplicative* and/or *additive* message signals depending on $\mathbf{B}_m(\mathbf{x})$. If $\mathbf{B}_m(\mathbf{x}) = \mathbf{B}_m$, where \mathbf{B}_m is a constant matrix, then (3) is a system with only *additive* messages.

The following three chaotic systems in the form of (3) will be utilized for designing chaotic communication systems in this chapter.

(1) Rossler system [47]

The Rossler system described by

$$\dot{\mathbf{x}} = \mathbf{f}(\mathbf{x}) = \begin{bmatrix} -x_2 - x_3 \\ x_1 + ax_2 \\ -cx_3 + x_1x_3 + b \end{bmatrix} \quad (4)$$

can be modified by chaotic parameter modulation resulting in a system with *state-dependent* (*multiplicative*) and *additive* messages as

$$\begin{cases} \dot{\mathbf{x}} = \mathbf{f}(\mathbf{x}, \mathbf{m}) = \begin{bmatrix} -x_2 - x_3 \\ x_1 + ax_2 \\ -(c - m_1)x_3 + x_1x_3 + (b + m_2) \end{bmatrix} = \begin{bmatrix} 0 & -1 & -1 \\ 1 & a & 0 \\ 0 & 0 & -c \end{bmatrix} \mathbf{x} + \begin{bmatrix} 0 \\ 0 \\ m_1x_3 + x_1x_3 + b \end{bmatrix} + \begin{bmatrix} 0 & 0 \\ 0 & 0 \\ 0 & 1 \end{bmatrix} \mathbf{m}, \\ \dot{\mathbf{m}} = \mathbf{A}_m \mathbf{m}, \\ \mathbf{y} = \mathbf{h}(\mathbf{x}, \mathbf{m}), \end{cases} \quad (5)$$

where $\Psi = \mathbf{0}$, and the chaotic parameters are given by $\{a, b, c\} = \{0.2, 0.2, 5.7\}$ [43] or $\{0.398, 2, 4\}$ [42]. Note that the Rossler system (4) contains only one nonlinear term. See also [48] for more details.

(2) Genesio-Tesi system [49]

The Genesio-Tesi system given by

$$\dot{\mathbf{x}} = \mathbf{f}(\mathbf{x}) = \begin{bmatrix} x_2 \\ x_3 \\ -cx_1 - bx_2 - ax_3 + x_1^2 \end{bmatrix} \quad (6)$$

can be modified in the form of (3) with state-dependent and additive message signals as,

$$\begin{cases} \dot{\mathbf{x}} = \mathbf{f}(\mathbf{x}, \mathbf{m}) = \begin{bmatrix} x_2 \\ x_3 + m_1 \\ -cx_1 - (b - m_1)x_2 - ax_3 + x_1^2 + m_2 \end{bmatrix} = \mathbf{f}(\mathbf{x}) + \begin{bmatrix} 0 \\ 0 \\ -x_2 \end{bmatrix} m_1 + \begin{bmatrix} 0 & 0 \\ 1 & 0 \\ 0 & 1 \end{bmatrix} \begin{bmatrix} m_1 \\ m_2 \end{bmatrix}, \\ \dot{\mathbf{m}} = \mathbf{A}_m \mathbf{m}, \\ \mathbf{y} = \mathbf{h}(\mathbf{x}, \mathbf{m}), \end{cases} \quad (7)$$

where $\Psi = \mathbf{0}$, a , b and c are the chaotic parameters satisfying $ab < c$ and are given by $\{a, b, c\} = \{1.2, 2.92, 5.7\}$ [49]. Note that, without the nonlinear term x_1^2 , the Genesio-Tesi system (6) is a linear time-invariant (LTI) system and is a state-space realization of the transfer function $G(s) = 1/(s^3 + as^2 + bs + c)$.

(3) Chua circuit [50]

The Chua circuit

$$\dot{\mathbf{x}} = \mathbf{f}(\mathbf{x}) = \begin{bmatrix} \alpha(x_2 - x_1^3 - cx_1) \\ x_1 - x_2 + x_3 \\ -\beta x_2 \end{bmatrix} \quad (8)$$

may be modulated in a form with state-dependent and additive messages as

$$\begin{cases} \dot{\mathbf{x}} = \mathbf{f}(\mathbf{x}, \mathbf{m}) = \begin{bmatrix} \alpha(x_2 - x_1^3 - cx_1) + m_1 \\ x_1 - x_2 + x_3 \\ -(\beta + m_2)x_2 \end{bmatrix} = \mathbf{f}(\mathbf{x}) + \begin{bmatrix} 1 \\ 0 \\ 0 \end{bmatrix} m_1 + \begin{bmatrix} 0 \\ 0 \\ -x_2 \end{bmatrix} m_2, \\ \dot{m} = A_m m, \\ \mathbf{y} = \mathbf{h}(\mathbf{x}, m), \end{cases} \quad (9)$$

where $\alpha = 10$, $\beta = 16$ and $c = -0.14$ are the chaotic parameters. A different modification scheme is given in Ref. [51].

It is noted that, although chaotic systems are sensitive to variations of their chaotic parameters $\mathbf{p} = \{p_i\}$, most systems do accommodate suitable modifications of some of these parameters. This property has precisely been exploited for the designs of UIOs for secure communication and many control-based synchronization schemes in the literature.

3. General unknown-input observers (UIOs)

Consider (3), which can be expressed more compactly as,

$$\begin{cases} \dot{\mathbf{w}} = \mathbf{f}_w(\mathbf{w}), \\ \mathbf{y} = \mathbf{h}(\mathbf{w}), \end{cases} \quad (10)$$

where

$$\mathbf{w} = \begin{bmatrix} \mathbf{x} \\ \mathbf{m} \end{bmatrix}, \mathbf{f}_w(\mathbf{w}) = \begin{bmatrix} \mathbf{f}(\mathbf{x}, \mathbf{m}) \\ \mathbf{f}_m(\mathbf{m}, \mathbf{x}) \end{bmatrix}, \text{ and } \mathbf{h}(\mathbf{w}) = \mathbf{h}(\mathbf{x}, \mathbf{m}).$$

Consider a Luenberger-like nonlinear observer for (3) given by [27–31, 34],

$$\begin{cases} \begin{bmatrix} \dot{\hat{\mathbf{x}}} \\ \dot{\hat{\mathbf{m}}} \end{bmatrix} = \begin{bmatrix} \mathbf{f}(\hat{\mathbf{x}}, \hat{\mathbf{m}}) \\ \mathbf{f}_m(\hat{\mathbf{m}}, \hat{\mathbf{x}}) \end{bmatrix} + \begin{bmatrix} \mathbf{L}_{1o}(\cdot) \\ \mathbf{L}_{2o}(\cdot) \end{bmatrix} [\mathbf{y} - \mathbf{h}(\hat{\mathbf{x}}, \hat{\mathbf{m}})], \\ \mathbf{y} = \mathbf{h}(\mathbf{x}, \mathbf{m}), \end{cases} \quad (11)$$

or more compactly as, with (10),

$$\begin{cases} \dot{\hat{\mathbf{w}}} = \mathbf{f}_w(\hat{\mathbf{w}}) + \mathbf{L}_o(\cdot) [\mathbf{y} - \mathbf{h}(\hat{\mathbf{w}})], \\ \mathbf{y} = \mathbf{h}(\mathbf{w}), \end{cases} \quad (12)$$

where $\hat{\mathbf{w}} = \begin{bmatrix} \hat{\mathbf{x}} \\ \hat{\mathbf{m}} \end{bmatrix}$ is an estimate of $\mathbf{w} = \begin{bmatrix} \mathbf{x} \\ \mathbf{m} \end{bmatrix}$, $\mathbf{f}_w(\hat{\mathbf{w}}) = \begin{bmatrix} \mathbf{f}(\hat{\mathbf{x}}, \hat{\mathbf{m}}) \\ \mathbf{f}_m(\hat{\mathbf{m}}, \hat{\mathbf{x}}) \end{bmatrix}$, and $\mathbf{L}_o(\cdot) = \begin{bmatrix} \mathbf{L}_{1o}(\cdot) \\ \mathbf{L}_{2o}(\cdot) \end{bmatrix}$ is the observer gain matrix to be determined such that the observer has desirable properties, such as generating an estimate $\hat{\mathbf{w}}(t)$ that can track (or converge to) $\mathbf{w}(t)$ asymptotically in the face of unknown disturbances.

Although (11) and (12) provide a more intuitive form for a Luenberger-like observer, a linear and nonlinear UIO can be expressed in an alternate form as [31, 52],

$$\begin{cases} \dot{\mathbf{q}} = \mathbf{f}_q(\mathbf{q}, \mathbf{y}), & \mathbf{q}(0) = \mathbf{q}_0, \\ \dot{\hat{\mathbf{w}}} = \boldsymbol{\varphi}(\mathbf{q}, \mathbf{y}), & \hat{\mathbf{w}} = \begin{bmatrix} \hat{\mathbf{x}} \\ \hat{\mathbf{m}} \end{bmatrix}, \end{cases} \quad (13)$$

where $\mathbf{q} \in \mathbb{R}^n$, $\mathbf{f}_q : \mathbb{R}^n \times \mathbb{R}^m \rightarrow \mathbb{R}^n$ is a smooth vector field, $\boldsymbol{\varphi}$ a smooth function, $\mathbf{f}_q(\mathbf{0}, \mathbf{0}) = \mathbf{0}$ and $\boldsymbol{\varphi}(\mathbf{0}, \mathbf{0}) = \mathbf{0}$.

Three classes of UIOs can be distinguished from the extended state estimate $\hat{\mathbf{w}}$, namely, (i) if $\hat{\mathbf{w}} = \begin{bmatrix} \hat{\mathbf{x}} \\ \hat{\mathbf{m}} \end{bmatrix}$, then (13) is a *full-order UIO* that addresses the estimation of the entire system vector \mathbf{x} and message vector \mathbf{m} ; (ii) if $\hat{\mathbf{w}} = \begin{bmatrix} \hat{\mathbf{x}}_2 \\ \hat{\mathbf{m}} \end{bmatrix}$, where $\hat{\mathbf{x}} = \begin{bmatrix} \mathbf{x}_1 \\ \hat{\mathbf{x}}_2 \end{bmatrix}$, \mathbf{x}_1 is known and $\hat{\mathbf{x}}_2$ is an estimate of \mathbf{x}_2 , then (13) is a *reduced-order UIO* that deals with partial-state and message estimations; and (iii) if $\hat{\mathbf{w}} = \hat{\mathbf{m}}$, where the complete state vector $\mathbf{x}(t)$ is known for all t , then (13) is an UIO for only message estimation.

The design of all the three classes of UIOs discussed above for secure communication will be addressed in Section 4.

4. Unknown-input observers (UIOs) for chaotic secure communication

The analysis and design of UIOs for secure communication using a drive-response scheme in this section will be based on (10)–(13). Hence, (3) or (10) will serve as the drive system, while (11), (12) or (13) as the response system.

In the drive-response chaotic communication theory and applications, one of the most important issues is *synchronization*, which is closely related to the stability of the UIO. Synchronization is a property of the estimation error $\tilde{\mathbf{w}}$ given by

$$\tilde{\mathbf{w}} = \begin{bmatrix} \tilde{\mathbf{x}} \\ \tilde{\mathbf{m}} \end{bmatrix}, \quad (14)$$

where $\tilde{\mathbf{x}} = \mathbf{x} - \hat{\mathbf{x}}$ and $\tilde{\mathbf{m}} = \mathbf{m} - \hat{\mathbf{m}}$.

Definition 1: Synchronization

The drive system (3) or (10) and the UIO response system (11), (12) or (13) are said to be *synchronized* if the estimation error $\tilde{\mathbf{w}}$ given by (14) satisfies $\lim_{t \rightarrow \infty} \|\tilde{\mathbf{w}}(t)\| = \lim_{t \rightarrow \infty} \|\mathbf{w}(t) - \hat{\mathbf{w}}(t)\| = 0$,

i.e., the UIO is capable of generating an estimate $\hat{\mathbf{w}}(t)$ that tracks $\mathbf{w}(t)$ asymptotically as $t \rightarrow \infty$. ■

Remark 1: The condition $\lim_{t \rightarrow \infty} \|\tilde{\mathbf{w}}(t)\| = 0$ is similar to the design of linear and nonlinear observers where it is crucial to ensure the asymptotic stability of the observers. ■

To proceed, the estimation error (14) satisfies, with (10) and (12),

$$\begin{aligned}\dot{\tilde{\mathbf{w}}} &= \mathbf{f}_w(\mathbf{w}) - \mathbf{f}_w(\hat{\mathbf{w}}) - \mathbf{L}_o(\cdot)[\mathbf{y} - \mathbf{h}(\hat{\mathbf{w}})] \\ &= \mathbf{f}_w(\mathbf{w}) - \mathbf{f}_w(\mathbf{w} - \tilde{\mathbf{w}}) - \mathbf{L}_o(\cdot)[\mathbf{h}(\mathbf{w}) - \mathbf{h}(\mathbf{w} - \tilde{\mathbf{w}})] \\ &\triangleq \mathbf{f}_w(\tilde{\mathbf{w}}, \mathbf{x}, \mathbf{m}, \mathbf{y}).\end{aligned}\quad (15)$$

It follows that $\tilde{\mathbf{w}} = \mathbf{0}$ is an equilibrium point of (15), i.e., $\mathbf{f}_w(\mathbf{w}) - \mathbf{f}_w(\mathbf{w}) - \mathbf{L}_o(\cdot)[\mathbf{h}(\mathbf{w}) - \mathbf{h}(\mathbf{w})] = \mathbf{f}_w(\mathbf{0}, \mathbf{x}, \mathbf{m}, \mathbf{y}) = \mathbf{0}$ for all \mathbf{x} , \mathbf{m} and \mathbf{y} . Further, if a gain $\mathbf{L}_o(\cdot)$ can be found such that (15) is asymptotically stable, then $\lim_{t \rightarrow \infty} [\hat{\mathbf{w}}(t)] = \lim_{t \rightarrow \infty} [\mathbf{w}(t)]$, see for example [29].

The results above are stated in the following theorem.

Theorem 1: Consider the error Eq. (15) with an equilibrium point at $\tilde{\mathbf{w}} = \mathbf{0}$. If a gain matrix $\mathbf{L}_o(\cdot)$ exists such that (15) is asymptotically stable, then $\hat{\mathbf{w}}(t) \rightarrow \mathbf{w}(t)$ as $t \rightarrow \infty$. ■

The next task is to determine the gain $\mathbf{L}_o(\cdot)$ so that the candidate observer (12) or (13) becomes an asymptotically or exponentially stable observer. The matrix can take on various forms depending on the type of systems being considered and/or the design techniques. For a general nonlinear system, $\mathbf{L}_o(\cdot)$ can be determined as a function of the estimate $\hat{\mathbf{x}}$, i.e., $\mathbf{L}_o(\cdot) = \mathbf{L}_o(\hat{\mathbf{x}})$ [27, 28]; for nonlinear systems under Jacobian linearization, $\mathbf{L}_o(\cdot)$ can be obtained as a constant matrix \mathbf{L}_o [29, 30]; for extended Kalman-Bucy filtering using Jacobian linearization, the filter gain matrix can be approximated by its steady-state value \mathbf{L}_o . We shall focus on Jacobian linearization in Section 4.1 below with applications to full-order UIOs for state and message estimations using constant gain $\mathbf{L}_o(\cdot) = \mathbf{L}_o$. Section 4.2 addresses the design of reduced-order UIOs for message estimation, while the design of reduced-order UIOs for partial-state and message estimations is considered in Section 4.3.

4.1. Jacobian linearization: full-order UIO

Linearization of (3) or (10) about the equilibrium point $\mathbf{w}^0 = \mathbf{0}$ yields

$$\bar{\mathbf{A}} = \left[\begin{array}{c|c} \mathbf{A} & \mathbf{B}_m \mathbf{M} \\ \hline \boldsymbol{\Psi} & \mathbf{A}_m \end{array} \right] \quad \text{and} \quad \bar{\mathbf{C}} = [\mathbf{C} \mid \mathbf{C}_m], \quad (16)$$

where

$$\begin{aligned}\mathbf{A} &= \left. \frac{\partial \mathbf{f}}{\partial \mathbf{x}}(\mathbf{x}, \mathbf{m}) \right|_{\mathbf{w}^0=0}, & \mathbf{B}_m \mathbf{M} &= \left. \frac{\partial \mathbf{f}}{\partial \mathbf{m}}(\mathbf{x}, \mathbf{m}) \right|_{\mathbf{w}^0=0}, & (\mathbf{B}_m &= \mathbf{B}_m(\mathbf{0})), & \boldsymbol{\Psi} &= \left. \frac{\partial \mathbf{f}_m}{\partial \mathbf{x}}(\mathbf{m}, \mathbf{x}) \right|_{\mathbf{w}^0=0}, \\ \mathbf{A}_m &= \left. \frac{\partial \mathbf{f}_m}{\partial \mathbf{m}}(\mathbf{m}, \mathbf{x}) \right|_{\mathbf{w}^0=0}, & \mathbf{C} &= \left. \frac{\partial \mathbf{h}}{\partial \mathbf{x}}(\mathbf{x}, \mathbf{m}) \right|_{\mathbf{w}^0=0}, & \mathbf{C}_m &= \left. \frac{\partial \mathbf{h}}{\partial \mathbf{m}}(\mathbf{x}, \mathbf{m}) \right|_{\mathbf{w}^0=0}.\end{aligned}$$

The resulting linearized system is given by

$$\begin{cases} \begin{bmatrix} \dot{\mathbf{x}} \\ \dot{\mathbf{m}} \end{bmatrix} = \bar{\mathbf{A}} \begin{bmatrix} \mathbf{x} \\ \mathbf{m} \end{bmatrix}, \\ \mathbf{y} = \bar{\mathbf{C}} \begin{bmatrix} \mathbf{x} \\ \mathbf{m} \end{bmatrix}. \end{cases} \quad (17)$$

The following assumption is crucial to the construction of UIOs.

Assumption 1: Observability

The pair $[\bar{\mathbf{A}}, \bar{\mathbf{C}}]$ in (17) is observable, i.e.,

$$\text{rank}[\mathcal{O}] = n + r,$$

where \mathcal{O} is the observability matrix

$$\mathcal{O} = \begin{bmatrix} \bar{\mathbf{C}}^T & \bar{\mathbf{A}}^T \bar{\mathbf{C}}^T & (\bar{\mathbf{A}}^2)^T \bar{\mathbf{C}}^T & \dots & (\bar{\mathbf{A}}^{(n+r-1)})^T \bar{\mathbf{C}}^T \end{bmatrix}. \quad \blacksquare$$

An observer can be constructed for (17) if and only if $[\bar{\mathbf{A}}, \bar{\mathbf{C}}]$ is an observable pair. Hence when the Jacobian linearization method yields a pair $[\bar{\mathbf{A}}, \bar{\mathbf{C}}]$ that is not observable, then the Jacobian linearization method is not applicable to the system under consideration. However, other methods may work, such as feedback linearization [53, 54].

Using (17), a linear UIO for full-state and message estimation can be constructed as

$$\begin{cases} \begin{bmatrix} \dot{\hat{\mathbf{x}}} \\ \dot{\hat{\mathbf{m}}} \end{bmatrix} = \bar{\mathbf{A}} \begin{bmatrix} \hat{\mathbf{x}} \\ \hat{\mathbf{m}} \end{bmatrix} + \begin{bmatrix} \mathbf{L}_{1o} \\ \mathbf{L}_{2o} \end{bmatrix} \left(\mathbf{y} - \bar{\mathbf{C}} \begin{bmatrix} \hat{\mathbf{x}} \\ \hat{\mathbf{m}} \end{bmatrix} \right) \\ \quad = (\bar{\mathbf{A}} - \mathbf{L}_o \bar{\mathbf{C}}) \begin{bmatrix} \hat{\mathbf{x}} \\ \hat{\mathbf{m}} \end{bmatrix} + \mathbf{L}_o \mathbf{y}, & \begin{bmatrix} \hat{\mathbf{x}}(0) \\ \hat{\mathbf{m}}(0) \end{bmatrix} = \begin{bmatrix} \hat{\mathbf{x}}_o \\ \hat{\mathbf{m}}_o \end{bmatrix}, \\ \mathbf{y} = \bar{\mathbf{C}} \begin{bmatrix} \mathbf{x} \\ \mathbf{m} \end{bmatrix}, \end{cases} \quad (18)$$

where $\mathbf{L}_o = \begin{bmatrix} \mathbf{L}_{1o} \\ \mathbf{L}_{2o} \end{bmatrix}$ is the constant UIO gain matrix to be determined. Note that $\mathbf{L}_{1o} \in \mathbb{R}^{n \times m}$ and $\mathbf{L}_{2o} \in \mathbb{R}^{r \times m}$, and (18) is simply a Luenberger observer [57]. Since $[\bar{\mathbf{A}}, \bar{\mathbf{C}}]$ is an observable pair by Assumption 1, then \mathbf{L}_o can be determined, for example, by pole-placement, such that $(\bar{\mathbf{A}} - \mathbf{L}_o \bar{\mathbf{C}})$ is Hurwitz, i.e., all the eigenvalues of $(\bar{\mathbf{A}} - \mathbf{L}_o \bar{\mathbf{C}})$ are located in the open left half-complex plane.

Using (17) and (18), the estimation errors $\tilde{\mathbf{x}} = \mathbf{x} - \hat{\mathbf{x}}$ and $\tilde{\mathbf{m}} = \mathbf{m} - \hat{\mathbf{m}}$ satisfy

$$\begin{bmatrix} \dot{\tilde{\mathbf{x}}} \\ \dot{\tilde{\mathbf{m}}} \end{bmatrix} = (\bar{\mathbf{A}} - \mathbf{L}_o \bar{\mathbf{C}}) \begin{bmatrix} \tilde{\mathbf{x}} \\ \tilde{\mathbf{m}} \end{bmatrix}, \quad \begin{bmatrix} \tilde{\mathbf{x}}(0) \\ \tilde{\mathbf{m}}(0) \end{bmatrix} = \begin{bmatrix} \tilde{\mathbf{x}}_o \\ \tilde{\mathbf{m}}_o \end{bmatrix}, \quad (19)$$

which is exponentially stable, i.e., $\lim_{t \rightarrow \infty} [\tilde{\mathbf{x}}(t)] = \mathbf{0}$ and $\lim_{t \rightarrow \infty} [\tilde{\mathbf{m}}(t)] = \mathbf{0}$ exponentially for all $\tilde{\mathbf{x}}(0)$ and $\tilde{\mathbf{m}}(0)$. It follows that $\hat{\mathbf{x}}(t) \rightarrow \mathbf{x}(t)$ and $\hat{\mathbf{m}}(t) \rightarrow \mathbf{m}(t)$ exponentially.

Once a constant \mathbf{L}_o has been determined, it can then be substituted into (12), whereby the resulting nonlinear UIO has the form

$$\begin{cases} \dot{\hat{\mathbf{w}}} = \mathbf{f}_w(\hat{\mathbf{w}}) + \mathbf{L}_o [\mathbf{y} - \mathbf{h}(\hat{\mathbf{w}})], & \hat{\mathbf{w}}(0) = \hat{\mathbf{w}}_o, \\ \mathbf{y} = \mathbf{h}(\hat{\mathbf{w}}), \end{cases} \quad (20)$$

where $\hat{\mathbf{w}}(0)$ is an arbitrary initial condition. Further, (15) becomes

$$\begin{aligned}\dot{\tilde{\mathbf{w}}} &= \mathbf{f}_w(\mathbf{w}) - \mathbf{f}_w(\hat{\mathbf{w}}) - \mathbf{L}_o[\mathbf{y} - \mathbf{h}(\hat{\mathbf{w}})] \\ &= \mathbf{f}_w(\mathbf{w}) - \mathbf{f}_w(\mathbf{w} - \tilde{\mathbf{w}}) - \mathbf{L}_o[\mathbf{h}(\mathbf{w}) - \mathbf{h}(\mathbf{w} - \tilde{\mathbf{w}})],\end{aligned}\quad (21)$$

which can be linearized about $\tilde{\mathbf{w}} = \mathbf{0}$ to give (19). Hence the dynamics of (21) close to the origin are well described by (19) for sufficiently small $\|\hat{\mathbf{w}}(0)\|$ [30].

In summary, we have the following theorem.

Theorem 2: Let $[\bar{\mathbf{A}}, \bar{\mathbf{C}}]$ be an observable pair so that there exists a constant gain \mathbf{L}_o such that $(\bar{\mathbf{A}} - \mathbf{L}_o \bar{\mathbf{C}})$ in (19) is Hurwitz. Then (20) is an exponentially stable dynamical system for sufficiently small $\|\hat{\mathbf{w}}(0)\|$. Further, $\hat{x}_i(t) \rightarrow x_i(t)$ and $\hat{m}_i(t) \rightarrow m_i(t)$ imply that the drive system (10) and the UIO response system (20) are synchronized. ■

Using (10) and (20), the overall chaotic system-based UIO for full-state and message estimations under the Jacobin linearization scheme can be implemented as

$$\begin{cases} \dot{\mathbf{w}} = \mathbf{f}_w(\mathbf{w}), & \mathbf{w}(0) = \mathbf{w}_o, \\ \dot{\hat{\mathbf{w}}} = \mathbf{f}_w(\hat{\mathbf{w}}) + \mathbf{L}_o[\mathbf{y} - \mathbf{h}(\hat{\mathbf{w}})], & \hat{\mathbf{w}}(0) = \hat{\mathbf{w}}_o, \\ \mathbf{y} = \mathbf{h}(\mathbf{x}, \mathbf{m}). \end{cases}\quad (22)$$

A block diagram for (22) is shown in **Figure 1**.

Example 1: Rossler system [47]

Consider the Rossler system with state-dependent and additive messages described by (5), with the output arranged as $\mathbf{y} = [x_1 + m_1 \quad x_3 + m_1]^T$,

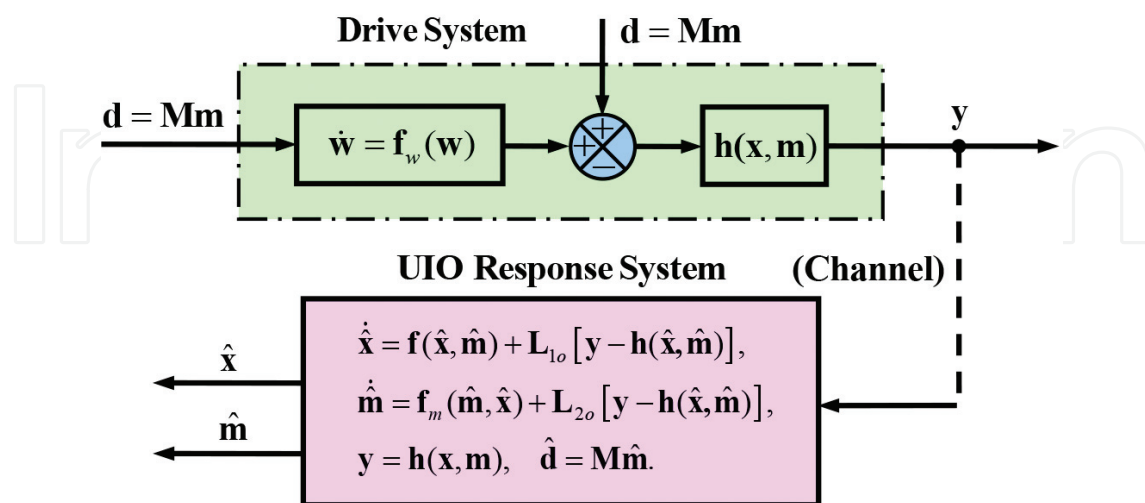


Figure 1. Chaotic secure communication system under Jacobian linearization.

$$\begin{cases} \dot{\mathbf{x}} = \begin{bmatrix} -x_2 - x_3 \\ x_1 + ax_2 \\ -(c - m_1)x_3 + x_1x_3 + (b + m_2) \end{bmatrix} = \underbrace{\begin{bmatrix} 0 & -1 & -1 \\ 1 & a & 0 \\ 0 & 0 & -c \end{bmatrix}}_{\mathbf{A}} \mathbf{x} + \underbrace{\begin{bmatrix} 0 \\ 0 \\ m_1x_3 + x_1x_3 + b \end{bmatrix}}_{\mathbf{g}(\mathbf{x}, m_1)} + \underbrace{\begin{bmatrix} 0 & 0 \\ 0 & 0 \\ 0 & 1 \end{bmatrix}}_{\mathbf{B}_m} \mathbf{m}, \\ \dot{\mathbf{m}} = \mathbf{A}_m \mathbf{m}, \\ \mathbf{y} = \begin{bmatrix} x_1 + m_1 \\ x_3 + m_1 \end{bmatrix} = \bar{\mathbf{C}} \begin{bmatrix} \mathbf{x} \\ \mathbf{m} \end{bmatrix}, \left(\bar{\mathbf{C}} = [\mathbf{C} \quad \mathbf{C}_m], \mathbf{C} = \begin{bmatrix} 1 & 0 & 0 \\ 0 & 0 & 1 \end{bmatrix}, \mathbf{C}_m = \begin{bmatrix} 1 & 0 \\ 1 & 0 \end{bmatrix} \right). \end{cases} \quad (23)$$

The preceding equation can be expressed as

$$\begin{cases} \begin{bmatrix} \dot{\mathbf{x}} \\ \dot{\mathbf{m}} \end{bmatrix} = \underbrace{\begin{bmatrix} \mathbf{A} & \mathbf{B}_m \\ \mathbf{0} & \mathbf{A}_m \end{bmatrix}}_{\bar{\mathbf{A}}} \begin{bmatrix} \mathbf{x} \\ \mathbf{m} \end{bmatrix} + \begin{bmatrix} \mathbf{g}(\mathbf{x}, m_1) \\ \mathbf{0} \end{bmatrix}, \\ \mathbf{y} = \begin{bmatrix} x_1 + m_1 \\ x_3 + m_1 \end{bmatrix} = \bar{\mathbf{C}} \begin{bmatrix} \mathbf{x} \\ \mathbf{m} \end{bmatrix}, \end{cases} \quad (24)$$

where $\mathbf{A}_m = \mathbf{0}$ for simplicity. Note that $[\bar{\mathbf{A}}, \bar{\mathbf{C}}]$ is an observable pair for all \mathbf{A}_m .

It can be shown that the Rossler system $\dot{\mathbf{x}} = \mathbf{f}(\mathbf{x})$ given by (4) has two equilibrium points, for $c^2 - 4ab \geq 0$,

$$\mathbf{x}_1^o = \begin{bmatrix} \frac{1}{2}(c + \sqrt{c^2 - 4ab}) \\ \frac{1}{2a}(-c - \sqrt{c^2 - 4ab}) \\ \frac{1}{2a}(c + \sqrt{c^2 - 4ab}) \end{bmatrix} = \begin{bmatrix} 5.693 \\ -28.465 \\ 28.465 \end{bmatrix}, \quad \mathbf{x}_2^o = \begin{bmatrix} \frac{1}{2}(c - \sqrt{c^2 - 4ab}) \\ \frac{1}{2a}(-c + \sqrt{c^2 - 4ab}) \\ \frac{1}{2a}(c - \sqrt{c^2 - 4ab}) \end{bmatrix} = \begin{bmatrix} 0.0070262 \\ -0.035131 \\ 0.035131 \end{bmatrix}.$$

The stability status of \mathbf{x}_1^o and \mathbf{x}_2^o can be determined by checking the eigenvalues of the Jacobian matrices $\mathbf{A}_1^o = \frac{\partial \mathbf{f}}{\partial \mathbf{x}}(\mathbf{x}_1^o)$ and $\mathbf{A}_2^o = \frac{\partial \mathbf{f}}{\partial \mathbf{x}}(\mathbf{x}_2^o)$. We obtain,

$$\frac{\partial \mathbf{f}}{\partial \mathbf{x}}(\mathbf{x}) = \begin{bmatrix} 0 & -1 & -1 \\ 1 & a & 0 \\ x_3 & 0 & x_1 - c \end{bmatrix} \Rightarrow \mathbf{A}_1^o = \begin{bmatrix} 0 & -1 & -1 \\ 1 & a & 0 \\ 28.465 & 0 & -0.007 \end{bmatrix} \text{ and } \mathbf{A}_2^o = \begin{bmatrix} 0 & -1 & -1 \\ 1 & a & 0 \\ 0.035131 & 0 & -5.693 \end{bmatrix}.$$

It follows that \mathbf{A} , \mathbf{A}_1^o and \mathbf{A}_2^o are unstable matrices, since their eigenvalues have positive real parts. Since \mathbf{A} , \mathbf{A}_1^o and \mathbf{A}_2^o can all be used for the design of an UIO for full-state and message estimations, we shall choose \mathbf{A} in the sequel. Therefore, using (18) and (24), it follows that the UIO for full-state and message estimations has the form

$$\begin{cases} \begin{bmatrix} \dot{\hat{\mathbf{x}}} \\ \dot{\hat{\mathbf{m}}} \end{bmatrix} = \bar{\mathbf{A}} \begin{bmatrix} \hat{\mathbf{x}} \\ \hat{\mathbf{m}} \end{bmatrix} + \begin{bmatrix} \mathbf{g}(\hat{\mathbf{x}}, \hat{m}_1) \\ \mathbf{0} \end{bmatrix} + \begin{bmatrix} \mathbf{L}_{1o} \\ \mathbf{L}_{2o} \end{bmatrix} \left(\mathbf{y} - \bar{\mathbf{C}} \begin{bmatrix} \hat{\mathbf{x}} \\ \hat{\mathbf{m}} \end{bmatrix} \right), \\ \quad = (\bar{\mathbf{A}} - \mathbf{L}_o \bar{\mathbf{C}}) \begin{bmatrix} \hat{\mathbf{x}} \\ \hat{\mathbf{m}} \end{bmatrix} + \begin{bmatrix} \mathbf{g}(\hat{\mathbf{x}}, \hat{m}_1) \\ \mathbf{0} \end{bmatrix} + \mathbf{L}_o \mathbf{y}, \quad \begin{bmatrix} \hat{\mathbf{x}}(0) \\ \hat{\mathbf{m}}(0) \end{bmatrix} = \begin{bmatrix} \hat{\mathbf{x}}_o \\ \hat{\mathbf{m}}_o \end{bmatrix}, \\ \mathbf{y} = \bar{\mathbf{C}} \begin{bmatrix} \mathbf{x} \\ \mathbf{m} \end{bmatrix}, \end{cases} \quad (25)$$

where the gain \mathbf{L}_o is to be determined such that $(\bar{\mathbf{A}} - \mathbf{L}_o \bar{\mathbf{C}})$ is Hurwitz. The next task is then to find \mathbf{L}_o , which may be obtained by using the pole-placement or Kalman-Bucy filter design method. We shall use the Kalman-Bucy filter technique. We note that in the design of a Kalman-Bucy filter [55, 56], the known covariance matrices of the system noise and measurement noise are given by \mathbf{Q} and \mathbf{R} , respectively, where $\mathbf{Q} \geq \mathbf{0}$ and $\mathbf{R} > \mathbf{0}$. However, for the UIO design governed by (24) and (25), there are no system and measurement noises. Hence, the elements of the \mathbf{Q} and \mathbf{R} matrices can be treated as free design parameters to be chosen and adjusted such that the performance of the UIO is satisfactory. A general method for choosing \mathbf{Q} and \mathbf{R} is to set them as diagonal matrices $\mathbf{Q} = q_{ii} \mathbf{I}_n$ and $\mathbf{R} = r_{ii} \mathbf{I}_r$, where \mathbf{I}_n and \mathbf{I}_r are unit matrices, and adjust the values of the diagonal elements q_{ii} and r_{ii} until satisfactory responses are obtained. In general, given a set of $\{r_{ii}\}$, larger values of $\{q_{ii}\}$ will lead to larger observer gains that will place the observer poles deeper in the left half-complex plane.

The overall UIO for full-state and message estimations can be implemented as (see (22))

$$\begin{cases} \dot{\mathbf{x}} = \mathbf{A}\mathbf{x} + \mathbf{g}(\mathbf{x}, m_1) + \mathbf{B}_m \mathbf{m}, & \mathbf{x}(0) = \mathbf{x}_o, \\ \dot{\hat{\mathbf{x}}} = \mathbf{A}\hat{\mathbf{x}} + \mathbf{g}(\hat{\mathbf{x}}, \hat{m}_1) + \mathbf{B}_m \hat{\mathbf{m}} + \mathbf{L}_{1o} (\mathbf{y} - \bar{\mathbf{C}} \hat{\mathbf{y}}), & \hat{\mathbf{x}}(0) = \hat{\mathbf{x}}_o, \\ \dot{\hat{\mathbf{m}}} = \mathbf{A}_m \hat{\mathbf{m}} + \mathbf{L}_{2o} (\mathbf{y} - \bar{\mathbf{C}} \hat{\mathbf{y}}), & \hat{\mathbf{m}}(0) = \hat{\mathbf{m}}_o, \\ \mathbf{y} = \begin{bmatrix} x_1 + m_1 \\ x_3 + m_1 \end{bmatrix} = \bar{\mathbf{C}} \begin{bmatrix} \mathbf{x} \\ \mathbf{m} \end{bmatrix}, \end{cases} \quad (26)$$

where the messages m_1 and m_2 are injected into the Rossler system directly (see **Figure 1** also), thereby the message model $\dot{\mathbf{m}} = \mathbf{A}_m \mathbf{m}$ is omitted in (26); however, the model matrix \mathbf{A}_m is needed in the message observer equation (third equation).

The key task now is the determination of a suitable UIO gain \mathbf{L}_o based on (24) that yields acceptable performance. The design can be accomplished by using Matlab's **LQR** command as

$$[\mathbf{L} \ \mathbf{P} \ \mathbf{E} \ \mathbf{o}] = \text{lqr}(\mathbf{A}\mathbf{b}', \mathbf{C}\mathbf{b}', \mathbf{Q}, \mathbf{R}), \quad \mathbf{L}_o = \mathbf{L}',$$

where $\mathbf{A}\mathbf{b}$ and $\mathbf{C}\mathbf{b}$ denote $\bar{\mathbf{A}}$ and $\bar{\mathbf{C}}$, respectively; $\mathbf{L}_o = \mathbf{P}\bar{\mathbf{C}}^T \mathbf{R}^{-1}$; $\mathbf{E}\mathbf{o} = \lambda(\bar{\mathbf{A}} - \mathbf{L}_o \bar{\mathbf{C}})$; and \mathbf{P} is the solution of the algebraic Riccati equation (ARE)

$$\mathbf{0} = \mathbf{P}\bar{\mathbf{A}}^T + \bar{\mathbf{A}}\mathbf{P} - \mathbf{P}\bar{\mathbf{C}}^T \mathbf{R}^{-1} \bar{\mathbf{C}}\mathbf{P} + \mathbf{Q} = \mathbf{P}\bar{\mathbf{A}}^T + \bar{\mathbf{A}}\mathbf{P} - \mathbf{L}_o \mathbf{R} \mathbf{L}_o^T + \mathbf{Q},$$

where $\mathbf{A}_m = \mathbf{0}$ in $\bar{\mathbf{A}}$ (see (24)). The parameter matrices \mathbf{Q} and \mathbf{R} that produced a suitable \mathbf{L}_o were found to be given by, respectively, (note that the adjustment of \mathbf{Q} was nontrivial),

$$\mathbf{Q} = \text{diag}([0, 50, 1000, 5 * 10^7, 10^{12}]), \mathbf{R} = \text{diag}([0.01, 0.01]).$$

We obtain

$$\mathbf{L}_o = \begin{bmatrix} 0.99979 & -0.99977 & -1e+005 \\ -0.03355 & -0.02882 & -1884 + 1876.6i \\ -3688.8 & 3830.5 & -1884 - 1876.6i \\ 51810 & 48122 & -0.4 + 0.8i \\ -6.8055e+006 & 7.33E+06 & -0.4 - 0.8i \end{bmatrix}$$

Note that the eigenvalues $\lambda(\bar{\mathbf{A}} - \mathbf{L}_o\bar{\mathbf{C}})$ are spread apart widely and have two complex conjugate poles.

The performance of the UIO is displayed in **Figures 2** and **3**. The initial conditions used in the simulations were: $\mathbf{x}(0) = \hat{\mathbf{x}}(0) = [0.2 \quad -0.4 \quad -0.2]^T$ and $\hat{\mathbf{m}} = [0 \quad 0]^T$. The signals to be estimated are: (a) a voice message $m_1(t)$ injected into the drive system at $t = 100$, and (b) the electrocardiogram (ECG) $m_2(t)$ of a person. **Figure 2(a)** shows $m_1(t)$ and its estimate $\hat{m}_1(t)$, and **Figure 2(b)** shows $m_2(t)$ and $\hat{m}_2(t)$. The estimation errors were small, as can be seen from **Figure 2(c)** and **(d)**, where the plots of m_1 vs. \hat{m}_1 , and m_2 vs. \hat{m}_2 are displayed. The clean 45-degree trace in **Figure 2(c)** shows that the estimate $\hat{m}_1(t)$ of $m_1(t)$ is almost perfect, while **Figure 2(d)** shows that the estimation error $\tilde{m}_2(t) = m_2(t) - \hat{m}_2(t)$ was small. The synchronization of the drive-response systems is shown in **Figure 3(a)–(d)**, where $\{x_1(t), \hat{x}_1(t)\}$ and $\{x_2(t), \hat{x}_2(t)\}$ are shown; the clean 45-degree traces of $x_1(t)$ vs. $\hat{x}_1(t)$ and $x_2(t)$ vs. $\hat{x}_2(t)$ show that the synchronization was nearly perfect. Hence, we conclude that the overall synchronization of the drive-response systems and the message estimation ranges from satisfactory to excellent.

4.2. Reduced-order UIO for message estimation for completely known $\mathbf{x}(t)$

The objective here is to estimate the unknown message signal vector $\mathbf{m}(t)$ by assuming that the entire state vector \mathbf{x} is accessible by direct measurement, i.e., full-state measurement, and does not have to be estimated. Hence, without loss of generality, the output can be assumed to be given by $\mathbf{y} = \mathbf{x}$. This leads to the construction of a reduced-order UIO for message (disturbance) estimation. In general, a reduced-order observer based on full-state or partial-state measurement has an interesting structure and is an active area of research in the literature for system controls and disturbance estimation, see for example [24–26, 57–60]. The reduced-order UIO designed in this section for message estimation will be based on a *derived measurement* derived from $\mathbf{y} = \mathbf{x}$ and $\dot{\mathbf{y}} = \dot{\mathbf{x}}$; the results will be extended to partial-state and message estimations in Section 4.3.

Before launching into the design of UIOs for message estimation, let us consider a general disturbance estimation problem described by

$$\begin{cases} \dot{\mathbf{x}} = \mathbf{f}(\mathbf{x}) + \mathbf{B}_1(\mathbf{x})\mathbf{u} + \mathbf{B}_2(\mathbf{x})\mathbf{d}, \\ \mathbf{y} = \mathbf{x}, \end{cases} \quad (27)$$

where $\mathbf{x} \in \mathbb{R}^n$ is the state vector, $\mathbf{u} \in \mathbb{R}^\ell$ a known control input vector, $\mathbf{d} \in \mathbb{R}^r$ an unknown disturbance vector, and \mathbf{y} the measured or known output vector; $\mathbf{f}(\mathbf{x})$, $\mathbf{B}_1(\mathbf{x})$ and $\mathbf{B}_2(\mathbf{x})$ are known function and matrices of compatible dimensions. The unknown disturbance \mathbf{d} is assumed to be generated by

$$\dot{\mathbf{d}} = \mathbf{f}_d(\mathbf{d}, \mathbf{x}), \quad (28)$$

where $\mathbf{f}_d(\mathbf{0}, \mathbf{0}) = \mathbf{0}$.

The objective is to estimate the unknown disturbance \mathbf{d} using the output $\mathbf{y} = \mathbf{x}$. The following lemma shows that \mathbf{d} can be estimated based on a *derived measurement* instead of \mathbf{y} .

Lemma 1: Estimation of \mathbf{d} based on derived measurement

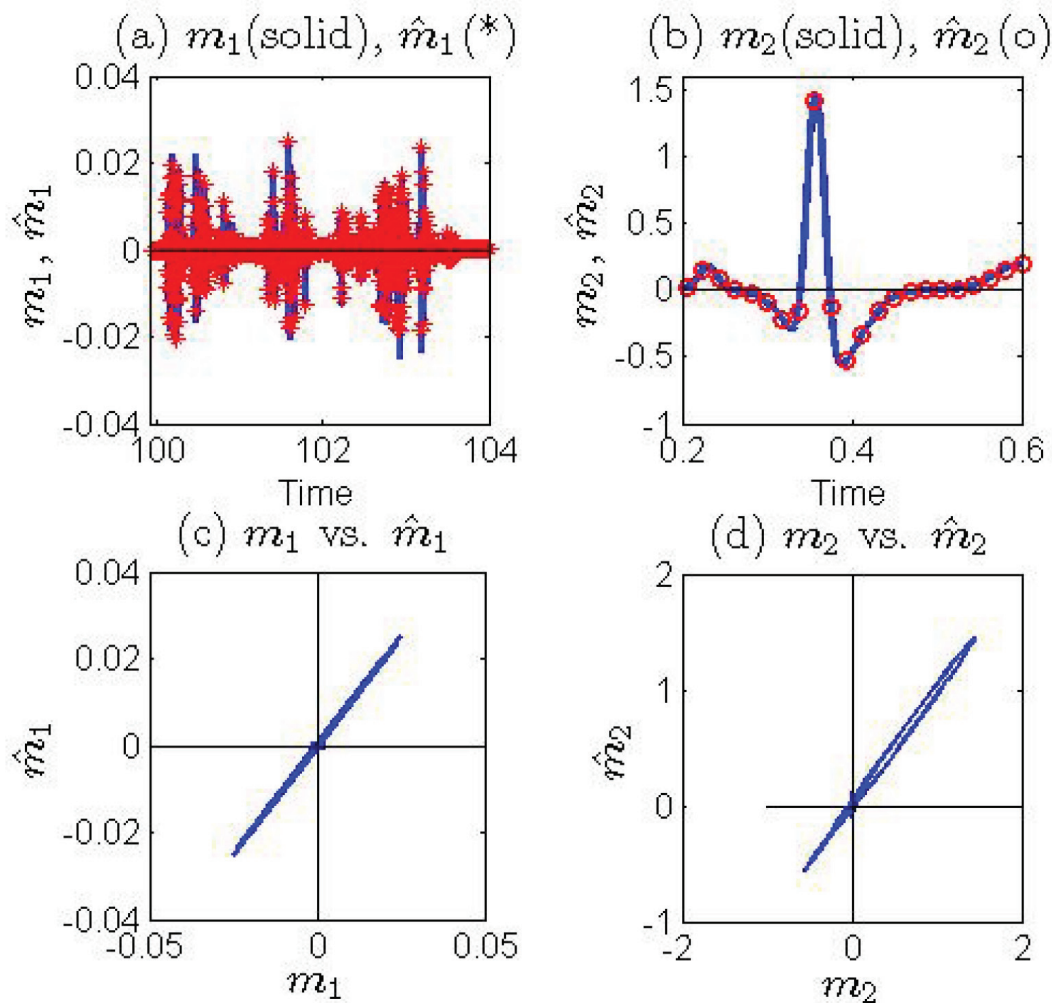


Figure 2. Responses of Rossler system: (a) m_1 and \hat{m}_1 ; (b) m_2 and \hat{m}_2 ; (c) m_1 vs. \hat{m}_1 ; and (d) m_2 vs. \hat{m}_2 . Figures 2(c) and 2(d) indicate negligible estimation error $\hat{m}_1 = m_1 - \hat{m}_1$ and small $\hat{m}_2 = m_2 - \hat{m}_2$, respectively.

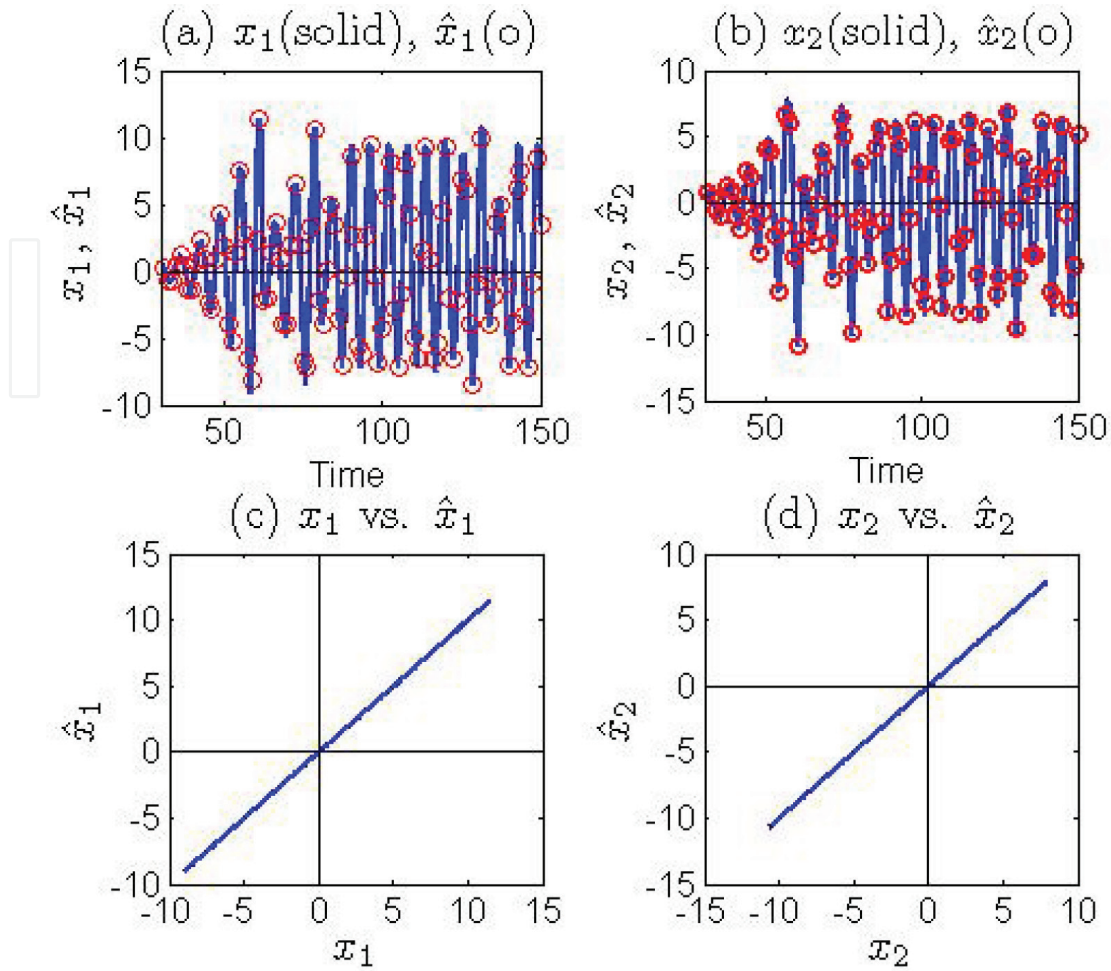


Figure 3. Responses of Rossler system: (a) x_1 and \hat{x}_1 ; (b) x_2 and \hat{x}_2 ; (c) x_1 vs. \hat{x}_1 ; and (d) x_2 vs. \hat{x}_2 . Figures 3(c) and 3(d) indicate negligible estimation errors $\tilde{x}_1 = x_1 - \hat{x}_1$ and $\tilde{x}_2 = x_2 - \hat{x}_2$, respectively.

Consider the systems described by (27) and (28). A Luenberger-like nonlinear observer can be constructed for disturbance estimation as

$$\dot{\hat{\mathbf{d}}} = \mathbf{f}_d(\hat{\mathbf{d}}, \mathbf{x}) + \mathbf{L}_o(\mathbf{x}) [\dot{\mathbf{x}} - \mathbf{f}(\mathbf{x}) - \mathbf{B}_1(\mathbf{x})\mathbf{u} - \mathbf{B}_2(\mathbf{x})\hat{\mathbf{d}}], \quad (29)$$

where $\hat{\mathbf{d}}$ is an estimate of \mathbf{d} , and $\mathbf{L}_o(\mathbf{x}) \in \mathbb{R}^{r \times n}$ is the observer gain to be determined such that $\hat{\mathbf{d}}(t) \rightarrow \mathbf{d}(t)$ asymptotically.

Proof: Define a derived measurement equation derived from the output $\mathbf{y} = \mathbf{x}$ as

$$\mathbf{y}_d = \dot{\mathbf{y}} - \mathbf{f}(\mathbf{x}) - \mathbf{B}_1(\mathbf{x})\mathbf{u}. \quad (30)$$

Since \mathbf{x} is known, $\dot{\mathbf{y}} = \dot{\mathbf{x}}$ can be obtained from its time derivative; hence $\mathbf{y}_d(t)$ is known for all $t \geq 0$ for known $\mathbf{f}(\mathbf{x})$ and $\mathbf{B}_1(\mathbf{x})\mathbf{u}$. Combining (28) and (30) yields, with (27),

$$\begin{cases} \dot{\hat{\mathbf{d}}} = \mathbf{f}_d(\hat{\mathbf{d}}, \mathbf{x}), \\ \mathbf{y}_d = \mathbf{B}_2(\mathbf{x})\hat{\mathbf{d}}, \end{cases} \quad (31)$$

which constitutes a standard form or “pattern” for constructing a nonlinear observer. Hence, a candidate Luenberger-like observer can be constructed for estimating \mathbf{d} based on \mathbf{y}_d (or simply by “pattern recognition”) as

$$\dot{\hat{\mathbf{d}}} = \mathbf{f}_d(\hat{\mathbf{d}}, \mathbf{x}) + \mathbf{L}_o(\mathbf{x}) [\mathbf{y}_d - \mathbf{B}_2(\mathbf{x})\hat{\mathbf{d}}]. \quad (32)$$

Substituting (30) into (32) yields (29). ■

Remark 2: When $\mathbf{f}_d(\hat{\mathbf{d}}, \mathbf{x}) = \mathbf{0}$, (29) is identical to the observer proposed in Ref. [61] (Eq. (3.2), p. 44) under a versatile *disturbance observer-based control (DOBC)* technique applicable to both linear and nonlinear systems. However, it is not clear how and why the derivative term $\dot{\mathbf{x}}$ shows up in their Eq. (3.2). In contrast, the formulation in Lemma 1 based on the method of *derived measurement* provides a clear insight, specifically, it clearly shows how $\dot{\mathbf{x}}$ finds its way into (29). Furthermore, since it is, in general, difficult to access the entire system state vector \mathbf{x} for measurement, the derived measurement formulation will pave the way for the design of reduced-order observers for joint partial-state and disturbance estimations (see Section 4.3) using only those state variables that are available by direct measurement, thereby extending the DOBC technique and applications. ■

Remark 3: The presence or origin of $\dot{\mathbf{y}}$ in a linear Luenberger observer is well known in the literature [57, 58]. It occurs in the construction of reduced-order linear observers, where the elimination of $\dot{\mathbf{y}}$ leads to the design of improved or enhanced reduced-order observers. As shown in (29), the derivative $\dot{\mathbf{y}}$ also occurs in constructing enhanced reduced-order nonlinear observers. ■

To continue further, the derivative $\dot{\mathbf{y}}$ in (29) can be eliminated by moving the term $\mathbf{L}(\mathbf{x})\dot{\mathbf{y}}$ to the left side of the equation to yield

$$\dot{\mathbf{z}} = [\mathbf{f}_d(\hat{\mathbf{d}}, \mathbf{x}) - \mathbf{L}_o(\mathbf{x})\mathbf{B}_2(\mathbf{x})\hat{\mathbf{d}}] - \mathbf{L}_o(\mathbf{x})[\mathbf{f}(\mathbf{x}) + \mathbf{B}_1(\mathbf{x})\mathbf{u}], \quad (33)$$

where $\mathbf{z} = \dot{\hat{\mathbf{d}}} - \mathbf{L}_o(\mathbf{x})\dot{\mathbf{y}}$. Defining [61],

$$\mathbf{z} = \dot{\hat{\mathbf{d}}} - \mathbf{p}(\mathbf{x})\dot{\mathbf{y}} \Rightarrow \dot{\mathbf{z}} = \dot{\hat{\mathbf{d}}} - \frac{\partial \mathbf{p}(\mathbf{x})}{\partial \mathbf{x}} \dot{\mathbf{y}} \Rightarrow \mathbf{L}_o(\mathbf{x}) = \frac{\partial \mathbf{p}(\mathbf{x})}{\partial \mathbf{x}}, \quad (34)$$

where $\mathbf{p}(\mathbf{x}) \in \mathbb{R}^{r \times n}$ is to be determined. If $\mathbf{f}_d(\hat{\mathbf{d}}, \mathbf{x}) = \mathbf{0}$, then (33) can be expressed as

$$\begin{cases} \dot{\mathbf{z}} = -\mathbf{L}_o(\mathbf{x})\mathbf{B}_2(\mathbf{x})\mathbf{z} - \mathbf{L}_o(\mathbf{x})[\mathbf{B}_2(\mathbf{x})\mathbf{p}(\mathbf{x}) + \mathbf{f}(\mathbf{x}) + \mathbf{B}_1(\mathbf{x})\mathbf{u}], \\ \hat{\mathbf{d}} = \mathbf{z} + \mathbf{p}(\mathbf{x})\mathbf{y}, \end{cases} \quad (35)$$

which is identical to the enhanced observer presented in Ref. [61] (see for example, Eq. (3.5), p. 44).

We now return to message estimation in chaotic systems. We can start with (3), which can be expressed as, with full-state measurement given by $\mathbf{y} = \mathbf{x}$,

$$\begin{cases} \dot{\mathbf{x}} = \mathbf{f}(\mathbf{x}) + \mathbf{B}_m(\mathbf{x})\mathbf{M}\mathbf{m}, \\ \dot{\mathbf{m}} = \mathbf{A}_m\mathbf{m} + \Psi\mathbf{x}, \\ \mathbf{y} = \mathbf{x}. \end{cases} \quad (36)$$

Since the entire state vector \mathbf{x} is known for all $t \geq 0$, (36) can be rearranged as

$$\begin{cases} \dot{\mathbf{m}} = \mathbf{A}_m\mathbf{m} + \Psi\mathbf{x}, \\ \mathbf{y}_d = \mathbf{B}_m(\mathbf{x})\mathbf{M}\mathbf{m}, \end{cases} \quad (37)$$

where

$$\mathbf{y}_d \triangleq \dot{\mathbf{y}} - \mathbf{f}(\mathbf{x}), \quad (\dot{\mathbf{y}} = \dot{\mathbf{x}}), \quad (38)$$

is the *derived-measurement* in the form of (30). Most importantly, \mathbf{y}_d can serve as the output equation for $\dot{\mathbf{m}} = \mathbf{A}_m\mathbf{m} + \Psi\mathbf{x}$, so that (37) provides a standard form or pattern for observer design. Accordingly, a candidate Luenberger-like observer can be constructed based on \mathbf{y}_d as

$$\begin{aligned} \dot{\hat{\mathbf{m}}} &= \mathbf{A}_m\hat{\mathbf{m}} + \Psi\mathbf{x} + \mathbf{L}_o(\mathbf{x})[\mathbf{y}_d - \mathbf{B}_m(\mathbf{x})\mathbf{M}\hat{\mathbf{m}}] \\ &= [\mathbf{A}_m - \mathbf{L}_o(\mathbf{x})\mathbf{B}_m(\mathbf{x})\mathbf{M}]\hat{\mathbf{m}} + \Psi\mathbf{x} + \mathbf{L}_o(\mathbf{x})[\dot{\mathbf{y}} - \mathbf{f}(\mathbf{x})], \quad \hat{\mathbf{m}}(0) = \hat{\mathbf{m}}_o, \end{aligned} \quad (39)$$

where $\mathbf{L}_o(\mathbf{x}) \in \mathbb{R}^{r \times n}$ is the observer gain matrix to be determined.

To proceed, it follows from (37) and (39) that the estimation error defined by $\tilde{\mathbf{m}} = \mathbf{m} - \hat{\mathbf{m}}$ satisfies

$$\dot{\tilde{\mathbf{m}}} = [\mathbf{A}_m - \mathbf{L}_o(\mathbf{x})\mathbf{B}_m(\mathbf{x})\mathbf{M}]\tilde{\mathbf{m}}, \quad \tilde{\mathbf{m}}(0) = \tilde{\mathbf{m}}_o, \quad (40)$$

which shows that if $\mathbf{L}_o(\mathbf{x})$ is a suitable stabilizing gain, then $\tilde{\mathbf{m}}(t)$ can be made to converge to zero asymptotically for arbitrary $\tilde{\mathbf{m}}(0)$, thereby $\hat{\mathbf{m}}(t) \rightarrow \mathbf{m}(t)$.

The results above are summarized in the following theorem.

Theorem 3: Consider (36)–(39). If there exists a gain $\mathbf{L}_o(\mathbf{x})$ such that (40) is asymptotically stable for all \mathbf{x} , then $\hat{\mathbf{m}}(t) \rightarrow \mathbf{m}(t)$ asymptotically. ■

Note that since $\mathbf{B}_m(\mathbf{x})$ is a function of \mathbf{x} , it complicates the determination of $\mathbf{L}_o(\mathbf{x})$ to achieve asymptotic stability. However, if $\mathbf{B}_m(\mathbf{x}) = \mathbf{B}_m$, where \mathbf{B}_m is a constant matrix, then $\mathbf{L}_o(\mathbf{x})$ can be determined as a constant \mathbf{L}_o , and can be computed by simple methods, such as pole placement, provided that $[\mathbf{A}_m, \mathbf{B}_m]$ is an observable pair (see Example 2 below).

Using (36), it follows that (35) takes on the form,

$$\begin{cases} \dot{\mathbf{z}} = [\mathbf{A}_m - \mathbf{L}_o(\mathbf{x})\mathbf{B}_m(\mathbf{x})\mathbf{M}]\mathbf{z} + \Psi\mathbf{x} + \mathbf{A}_m\mathbf{p}(\mathbf{x}) - \mathbf{L}_o(\mathbf{x})[\mathbf{B}_m(\mathbf{x})\mathbf{M}\mathbf{p}(\mathbf{x}) + \mathbf{f}(\mathbf{x})], \\ \hat{\mathbf{m}} = \mathbf{z} + \mathbf{p}(\mathbf{x}). \end{cases} \quad (41)$$

A main task in applying (41) is the determination of $\mathbf{p}(\mathbf{x})$. If we set $\mathbf{p}(\mathbf{x})$ as a linear function of \mathbf{x} , i.e.,

$$\mathbf{p}(\mathbf{x}) = \mathbf{L}_o \mathbf{x}, \quad (\mathbf{x} = \mathbf{y}), \quad (42)$$

where \mathbf{L}_o is a constant matrix, then we obtain from (34), $\mathbf{L}(\mathbf{x}) = \mathbf{L}_o$. Further, if $\mathbf{B}_m(\mathbf{x}) = \mathbf{B}_m$ and $[\mathbf{A}_m, \mathbf{B}_m \mathbf{M}]$ is an observable pair, then \mathbf{L}_o can be determined readily by, for example, the pole-placement method, such that $(\mathbf{A}_m - \mathbf{L}_o \mathbf{B}_m \mathbf{M})$ is Hurwitz. Moreover, (40) becomes,

$$\dot{\tilde{\mathbf{m}}} = (\mathbf{A}_m - \mathbf{L}_o \mathbf{B}_m \mathbf{M}) \tilde{\mathbf{m}}, \quad \tilde{\mathbf{m}}(0) = \tilde{\mathbf{m}}_o, \quad (43)$$

which shows that $\tilde{\mathbf{m}}(t) \rightarrow \mathbf{0}$, thereby $\hat{\mathbf{m}}(t) \rightarrow \mathbf{m}(t)$ exponentially for arbitrary $\tilde{\mathbf{m}}(0)$. In addition, in this case, the enhanced UIO (41) reduces to

$$\begin{cases} \dot{\mathbf{z}} = (\mathbf{A}_m - \mathbf{L}_o \mathbf{B}_m \mathbf{M}) \mathbf{z} + [(\mathbf{A}_m - \mathbf{L}_o \mathbf{B}_m \mathbf{M}) \mathbf{L}_o \mathbf{x} + \Psi \mathbf{x} - \mathbf{L}_o \mathbf{f}(\mathbf{x})], \\ \hat{\mathbf{m}} = \mathbf{z} + \mathbf{L}_o \mathbf{y}. \end{cases} \quad (44)$$

It can be shown that the preceding equation can be obtained by using the linearized system (17) and setting $\mathbf{p}(\mathbf{x}) = \mathbf{L}_o \mathbf{x} \Rightarrow \mathbf{L}_o = \partial \mathbf{p}(\mathbf{x}) / \partial \mathbf{x}$.

Once a suitable gain has been determined, such as $\mathbf{L}_o(\mathbf{x}) = \mathbf{L}_o$, it can then be substituted into (41), and the overall chaotic system-based UIO for message estimation can be implemented as, with (36),

$$\begin{cases} \dot{\mathbf{x}} = \mathbf{f}(\mathbf{x}) + \mathbf{B}_m(\mathbf{x}) \mathbf{M} \mathbf{m}, & \mathbf{x}(0) = \mathbf{x}_o, \\ \dot{\mathbf{m}} = \mathbf{A}_m \mathbf{m} + \Psi \mathbf{x}, & \mathbf{m}(0) = \mathbf{m}_o, \\ \dot{\mathbf{z}} = (\mathbf{A}_m - \mathbf{L}_o \mathbf{B}_m(\mathbf{x}) \mathbf{M}) \mathbf{z} + [(\mathbf{A}_m - \mathbf{L}_o \mathbf{B}_m(\mathbf{x}) \mathbf{M}) \mathbf{L}_o \mathbf{x} + \Psi \mathbf{x} - \mathbf{L}_o \mathbf{f}(\mathbf{x})], & \mathbf{z}(0) = \mathbf{z}_o, \\ \hat{\mathbf{m}} = \mathbf{z} + \mathbf{L}_o \mathbf{y}, \\ \mathbf{y} = \mathbf{x}. \end{cases} \quad (45)$$

We remark that the UIO governed by the third equation in (45) is a nonlinear observer with its gain $\mathbf{L}_o(\mathbf{x})$ replaced by a constant \mathbf{L}_o . Other methods may be used to determine a suitable \mathbf{L}_o , such as linear matrix inequality (LMI), see for example Ref. [34].

Example 2: Genesio-Tesi system [49]

Consider the Genesio-Tesi system described by (7) with additive messages and output $\mathbf{y} = \mathbf{x}$

$$\begin{cases} \dot{\mathbf{x}} = \begin{bmatrix} x_2 \\ x_3 + m_1 \\ -cx_1 - bx_2 - ax_3 + x_1^2 + m_2 \end{bmatrix} = \mathbf{f}(\mathbf{x}) + \underbrace{\begin{bmatrix} 0 & 0 \\ 1 & 0 \\ 0 & 1 \end{bmatrix}}_{\mathbf{B}_m} \begin{bmatrix} m_1 \\ m_2 \end{bmatrix}, \\ \dot{\mathbf{m}} = \mathbf{A}_m \mathbf{m}, \\ \mathbf{y} = \mathbf{x}. \end{cases} \quad (46)$$

Using (37) with $\Psi = \mathbf{0}$, the preceding equation can be arranged in the form of an LTI system as

$$\begin{cases} \dot{\mathbf{m}} = \mathbf{A}_m \mathbf{m}, \\ \mathbf{y}_d = \mathbf{B}_m \mathbf{m}, \end{cases} \quad (47)$$

where $\mathbf{y}_d = \dot{\mathbf{y}} - \mathbf{f}(\mathbf{x})$ is the derived measurement, and it can be shown that $[\mathbf{A}_m, \mathbf{B}_m]$ is an observable pair for all \mathbf{A}_m , i.e., $\text{rank}[\mathbf{B}_m^T \quad \mathbf{A}_m^T \mathbf{B}_m^T] = 2$.

An observer for (47) can be constructed as

$$\begin{aligned}\dot{\hat{\mathbf{m}}} &= \mathbf{A}_m \hat{\mathbf{m}} + \mathbf{L}_o (\mathbf{y}_d - \mathbf{L}_o \mathbf{B}_m \hat{\mathbf{m}}) \\ &= (\mathbf{A}_m - \mathbf{L}_o \mathbf{B}_m) \hat{\mathbf{m}} + \mathbf{L}_o [\dot{\mathbf{y}} - \mathbf{f}(\mathbf{x})],\end{aligned}\quad (48)$$

which is obtainable from (39). Since $[\mathbf{A}_m, \mathbf{B}_m]$ is an observable pair, a constant gain \mathbf{L}_o can be determined such that $(\mathbf{A}_m - \mathbf{L}_o \mathbf{B}_m)$ is Hurwitz. Further, eliminating the derivative term $\mathbf{L}_o \dot{\mathbf{y}}$ in (48) yields

$$\begin{cases} \dot{\mathbf{z}} = (\mathbf{A}_m - \mathbf{L}_o \mathbf{B}_m) \mathbf{z} + [(\mathbf{A}_m - \mathbf{L}_o \mathbf{B}_m) \mathbf{L}_o \mathbf{y} - \mathbf{L}_o \mathbf{f}(\mathbf{x})], \\ \hat{\mathbf{m}} = \mathbf{z} + \mathbf{L}_o \mathbf{y}. \end{cases}\quad (49)$$

To determine the gain \mathbf{L}_o , let the poles of $(\mathbf{A}_m - \mathbf{L}_o \mathbf{B}_m)$ be selected as $\mathbf{po} = -[61 \quad 32]$. Using Matlab's pole-placement command,

$$\mathbf{L}_o = \text{place}(\mathbf{A}_m', \mathbf{B}_m', \mathbf{po})',$$

we obtain, for $\mathbf{A}_m = \mathbf{0}$,

$\mathbf{L}_o = \mathbf{0}$	61	0
0	0	32

The final result for implementation can be obtained by combining Eqs. (46) and (49) as

$$\begin{cases} \dot{\mathbf{x}} = \mathbf{f}(\mathbf{x}) + \mathbf{B}_m \mathbf{m}, & \mathbf{x}(0) = \mathbf{x}_o, \\ \dot{\mathbf{z}} = (\mathbf{A}_m - \mathbf{L}_o \mathbf{B}_m) \mathbf{z} + [(\mathbf{A}_m - \mathbf{L}_o \mathbf{B}_m) \mathbf{L}_o \mathbf{y} - \mathbf{L}_o \mathbf{f}(\mathbf{x})], & \mathbf{z}(0) = \mathbf{z}_o, \\ \hat{\mathbf{m}} = \mathbf{z} + \mathbf{L}_o \mathbf{y}, \\ \mathbf{y} = \mathbf{x}. \end{cases}\quad (50)$$

Since $m_1(t)$ and $m_2(t)$ are injected directly into the Genesio-Tesi system (46), the message model $\dot{\mathbf{m}} = \mathbf{A}_m \mathbf{m}$ is not needed and is omitted in (50); however, the model matrix \mathbf{A}_m is required in the estimation equation (second equation in (50)). The signal $m_1(t)$ is the nine-term Fourier series of a square wave, and $m_2(t)$ is a mix signal consisting of a trapezoid, sine wave, and ramp and exponential functions. It would be difficult to generate these rather complicated signals, in particular $m_2(t)$, by using the simple model $\dot{\mathbf{m}} = \mathbf{A}_m \mathbf{m}$, and/or a more general model $\dot{\mathbf{m}} = \mathbf{A}_m \mathbf{m} + \delta$ proposed in Refs. [24–26], where the elements $\delta_i(t)$ of $\delta(t)$ are unknown sequences of random delta functions. For simulation studies, the mix signal $m_2(t)$ can easily be generated by the following Matlab codes and injected into (50):

Mix signal $m_2(t)$:

$$\begin{aligned}m2 = & 0.05 * t * ((t > 0) \& (t < 10)) + 0.5 * ((t \geq 10) \& (t \leq 20)) \\ & - 0.05 * (t - 30) * ((t > 20) \& (t \leq 30)) + 0.25 * \sin(t - 30) * ((t \geq 30) \& (t < 58.27))\end{aligned}$$

$$+ (1/20) * (t-58.27) * ((t \geq 58.27) \& (t < 78.27)) \\ + 1 * \exp(-0.2 * (t-78.27)) * ((t \geq 78.27) \& (t < 200)).$$

The performance of the UIO is displayed in **Figures 4** and **5**. The initial condition of the Genesio-Tesi system used in the simulation was $\mathbf{x}(0) = [0.2 \quad -0.4 \quad -0.2]^T$, while $\mathbf{z}(0)$ was calculated by using $\mathbf{z}(0) = \hat{\mathbf{m}}(0) - \mathbf{L}_o \mathbf{y}(0) = -\mathbf{L}_o \mathbf{x}(0)$, which yields $\mathbf{z}(0) = [24.4 \quad 6.4]^T$ where $\hat{\mathbf{m}}(0) = \mathbf{0}$. **Figure 4(a)** shows $m_1(t)$ and its estimate $\hat{m}_1(t)$, and **Figure 4(b)** exhibits $m_2(t)$ and $\hat{m}_2(t)$. The estimation errors were negligible, as can be seen from **Figure 4(c)** and **(d)**, where the plots of $m_1(t)$ vs. $\hat{m}_1(t)$, and $m_2(t)$ vs. $\hat{m}_2(t)$ are displayed. Note also the Gibb's phenomenon (the "twin-towers") in **Figure 4(a)**. The Genesio-Tesi attractor is shown in **Figure 5**. We conclude that the performance of the reduced-order UIO for message estimation was satisfactory.

4.3. Reduced-order UIO for partial-state and message estimations

The objective in this section is to extend the design of reduced-order UIO for message estimation to the design of UIO for joint partial-state and message estimations. The results obtained are believed to be new and novel.

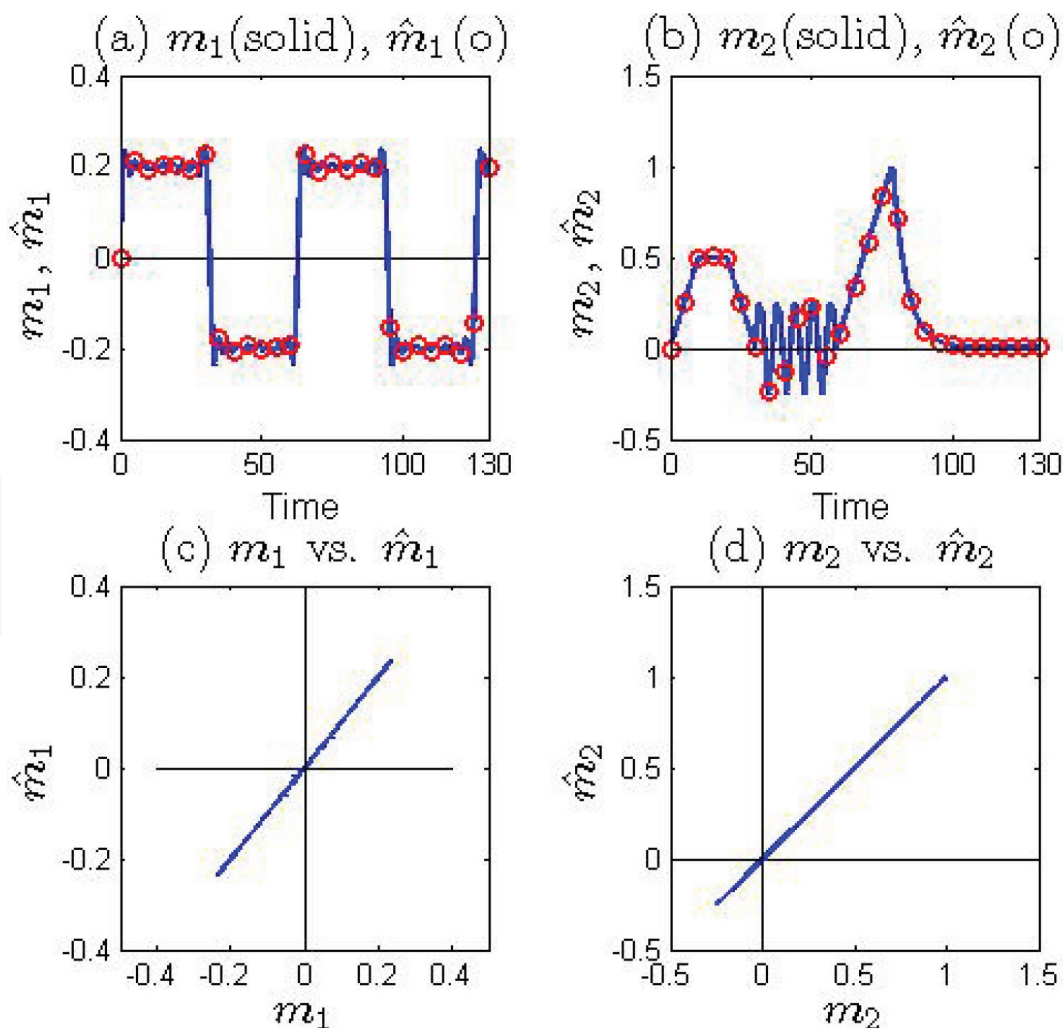


Figure 4. Responses of Genesio-Tesi system: (a) m_1 and \hat{m}_1 ; (b) m_2 and \hat{m}_2 ; (c) m_1 vs. \hat{m}_1 ; and (d) m_2 vs. \hat{m}_2 . Figures 4(c) and 4(d) indicate negligible estimation error $\tilde{m}_1 = m_1 - \hat{m}_1$ and $\tilde{m}_2 = m_2 - \hat{m}_2$, respectively.

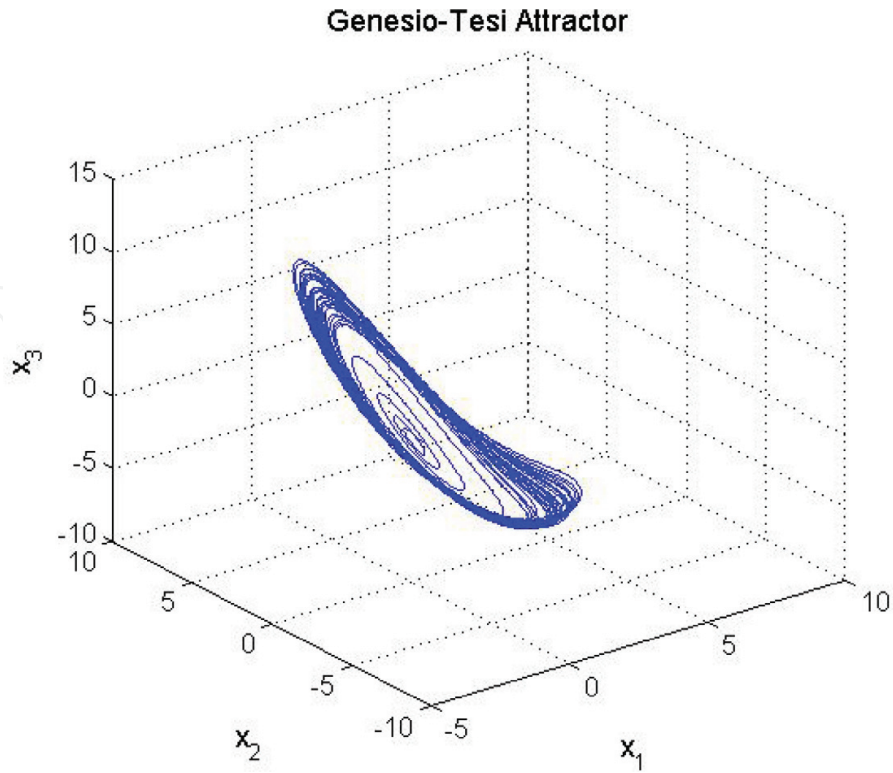


Figure 5. Genesio-Tesi attractor obtained by using (46).

Consider a general nonlinear system described by (3) which is expressed here without the output as (see also (1) and (2))

$$\begin{cases} \dot{\mathbf{x}} = \mathbf{f}(\mathbf{x}) + \mathbf{B}_m(\mathbf{x})\mathbf{M}\mathbf{m}, \\ \dot{\mathbf{m}} = \mathbf{A}_m\mathbf{m}, \end{cases} \quad (51)$$

where $\Psi = 0$. The design will be based on a derived measurement formulation.

Let

$$\mathbf{x} = \begin{bmatrix} \mathbf{x}_1 \\ \mathbf{x}_2 \end{bmatrix}, \quad \mathbf{w} \triangleq \begin{bmatrix} \mathbf{x}_2 \\ \mathbf{m} \end{bmatrix}, \quad \mathbf{y} = \mathbf{x}_1, \quad (52)$$

where $\mathbf{x}_1 \in \mathbb{R}^m$ and $\mathbf{x}_2 \in \mathbb{R}^{n-m}$ are, respectively, accessible and inaccessible for direct measurement, and \mathbf{y} is the output. Using (52), we assume that (51) can be partitioned as

$$\begin{cases} \dot{\mathbf{x}}_1 = \mathbf{f}_1(\mathbf{y}) + \mathbf{B}_{1m}(\mathbf{y})\mathbf{M}\mathbf{m}, & (\mathbf{y} = \mathbf{x}_1), \\ \dot{\mathbf{x}}_2 = \mathbf{f}_2(\mathbf{y}, \mathbf{x}_2, \mathbf{m}) + \mathbf{B}_{2m}(\mathbf{y}, \mathbf{x}_2)\mathbf{M}\mathbf{m}, \\ \dot{\mathbf{m}} = \mathbf{A}_m\mathbf{m}, \end{cases} \quad (53)$$

which can be rearranged to give

$$\begin{cases} \begin{bmatrix} \dot{\mathbf{x}}_2 \\ \dot{\mathbf{m}} \end{bmatrix} = \begin{bmatrix} \mathbf{f}_2(\mathbf{y}, \mathbf{x}_2, \mathbf{m}) \\ \mathbf{A}_m \mathbf{m} \end{bmatrix} + \begin{bmatrix} \mathbf{B}_{2m}(\mathbf{y}, \mathbf{x}_2) \mathbf{M} \mathbf{m} \\ \mathbf{0} \end{bmatrix}, \\ \mathbf{y}_d = \mathbf{B}_{1m}(\mathbf{y}) \mathbf{M} \mathbf{m}, \end{cases} \quad (54)$$

where $\mathbf{y}_d = \dot{\mathbf{y}} - \mathbf{f}_1(\mathbf{y})$ denotes the derived measurement.

Eq. (54) constitutes a standard form that can be used to construct an observer for estimating the inaccessible partial-state \mathbf{x}_2 and the unknown message \mathbf{m} based on the derived measurement \mathbf{y}_d . Hence, a candidate Luenberger-like observer can be constructed as

$$\dot{\hat{\mathbf{w}}} = \begin{bmatrix} \mathbf{f}_2(\mathbf{y}, \hat{\mathbf{x}}_2, \hat{\mathbf{m}}) \\ \mathbf{A}_m \hat{\mathbf{m}} \end{bmatrix} + \begin{bmatrix} \mathbf{B}_{2m}(\mathbf{y}, \hat{\mathbf{x}}_2) \mathbf{M} \hat{\mathbf{m}} \\ \mathbf{0} \end{bmatrix} + \begin{bmatrix} \mathbf{L}_{10}(\cdot) \\ \mathbf{L}_{20}(\cdot) \end{bmatrix} [\mathbf{y}_d - \mathbf{B}_{1m}(\mathbf{y}) \mathbf{M} \hat{\mathbf{m}}], \quad (55)$$

where $\mathbf{L}_{10}(\cdot)$ and $\mathbf{L}_{20}(\cdot)$ are the gain matrices to be determined such that the observer has desirable performance characteristics, in particular, $\hat{\mathbf{x}}_2(t) \rightarrow \mathbf{x}_2(t)$ and $\hat{\mathbf{m}}(t) \rightarrow \mathbf{m}(t)$ as $t \rightarrow \infty$.

Remark 4: In (39), the reduced-order UIO was derived using the output $\mathbf{y} = \mathbf{x}$, while the reduced-order UIO (55) above was constructed by using $\mathbf{y} = \mathbf{x}_1$ with \mathbf{x}_1 serving the role of \mathbf{x} . Hence (55) is an extension of the DOBC technique, and is now applicable to partial-state and message estimations by using only \mathbf{x}_1 instead of the entire state \mathbf{x} .

The estimation error $\tilde{\mathbf{w}} = [\tilde{\mathbf{x}}_2^T \quad \tilde{\mathbf{m}}^T]^T$, where $\tilde{\mathbf{x}}_2 = \mathbf{x}_2 - \hat{\mathbf{x}}_2$ and $\tilde{\mathbf{m}} = \mathbf{m} - \hat{\mathbf{m}}$, satisfies, with (54) and (55),

$$\dot{\tilde{\mathbf{w}}} = \begin{bmatrix} \mathbf{f}_2(\mathbf{y}, \mathbf{x}_2, \mathbf{m}) - \mathbf{f}_2(\mathbf{y}, \hat{\mathbf{x}}_2, \hat{\mathbf{m}}) \\ \mathbf{A}_m \mathbf{m} - \mathbf{A}_m \hat{\mathbf{m}} \end{bmatrix} + \begin{bmatrix} \mathbf{B}_{2m}(\mathbf{y}, \mathbf{x}_2) \mathbf{M} \mathbf{m} - \mathbf{B}_{2m}(\mathbf{y}, \hat{\mathbf{x}}_2) \mathbf{M} \hat{\mathbf{m}} \\ \mathbf{0} \end{bmatrix} - \begin{bmatrix} \mathbf{L}_{10}(\cdot) \\ \mathbf{L}_{20}(\cdot) \end{bmatrix} [\mathbf{y}_d - \mathbf{B}_{1m}(\mathbf{y}) \mathbf{M} \hat{\mathbf{m}}]. \quad (56)$$

The preceding error equation is a version of (15). Hence from Theorem 1, the origin $(\mathbf{0}, \mathbf{0})$ is an equilibrium point of the unforced equation in (56) for all $\mathbf{y} = \mathbf{x}_1$. Further, $\hat{\mathbf{x}}_2(t) \rightarrow \mathbf{x}_2(t)$ and $\hat{\mathbf{m}}(t) \rightarrow \mathbf{m}(t)$ if $\mathbf{L}_{10}(\cdot)$ and $\mathbf{L}_{20}(\cdot)$ are stabilizing gains.

The next task is to eliminate $\dot{\mathbf{y}}$ in $\mathbf{y}_d = \dot{\mathbf{y}} - \mathbf{f}_1(\mathbf{y})$ in (55) by moving $\mathbf{L}_o(\cdot)\dot{\mathbf{y}}$ to the left side of the equation and defining

$$\dot{\mathbf{z}} = \dot{\hat{\mathbf{w}}} - \mathbf{L}_o(\cdot)\dot{\mathbf{y}}. \quad (57)$$

Choosing

$$\mathbf{z} = \hat{\mathbf{w}} - \mathbf{p}(\mathbf{x}_1) \Rightarrow \dot{\mathbf{z}} = \dot{\hat{\mathbf{w}}} - \frac{\partial \mathbf{p}(\mathbf{x}_1)}{\partial \mathbf{x}_1} \dot{\mathbf{x}}_1, \quad (\dot{\mathbf{x}}_1 = \dot{\mathbf{y}}), \quad (58)$$

where $\mathbf{p}(\mathbf{x}_1) = \begin{bmatrix} \mathbf{p}_1(\mathbf{x}_1) \\ \mathbf{p}_2(\mathbf{x}_1) \end{bmatrix}$, $\mathbf{p}_1(\mathbf{x}_1) \in \mathbb{R}^{(n-m) \times (n-m)}$ and $\mathbf{p}_2(\mathbf{x}_1) \in \mathbb{R}^{r \times (n-m)}$ are to be determined. It follows that

$$\mathbf{L}_{1o}(\mathbf{x}_1) = \frac{\partial \mathbf{p}_1(\mathbf{x}_1)}{\partial \mathbf{x}_1} \quad \text{and} \quad \mathbf{L}_{2o}(\mathbf{x}_1) = \frac{\partial \mathbf{p}_2(\mathbf{x}_1)}{\partial \mathbf{x}_1} \quad (59)$$

Using (55), (57), (58) and (59), can be expressed as

$$\begin{cases} \dot{\mathbf{z}} = \begin{bmatrix} \mathbf{f}_2(\mathbf{y}, \hat{\mathbf{x}}_2, \hat{\mathbf{m}}) \\ \mathbf{A}_m \hat{\mathbf{m}} \end{bmatrix} + \begin{bmatrix} \mathbf{B}_{2m}(\mathbf{y}, \hat{\mathbf{x}}_2) \mathbf{M} \hat{\mathbf{m}} \\ \mathbf{0} \end{bmatrix} - \begin{bmatrix} \mathbf{L}_{1o}(\mathbf{x}_1) \\ \mathbf{L}_{2o}(\mathbf{x}_1) \end{bmatrix} [\mathbf{f}_1(\mathbf{y}) + \mathbf{B}_{1m}(\mathbf{y}) \mathbf{M} \hat{\mathbf{m}}], \\ \hat{\mathbf{w}} = \mathbf{z} + \mathbf{p}(\mathbf{x}_1), \end{cases} \quad (60)$$

which can further be reduced to a form given by, for example (44), once the specific structure of the chaotic system under consideration is known and $\mathbf{p}(\mathbf{x}_1)$ has been determined (see Example 3 for more details).

Using (51) and (60), the main results for the construction of UIO for partial-state and message estimations are stated in the following theorem.

Theorem 4: Consider the augmented system (54), where $\mathbf{y}_d = \mathbf{B}_{1m}(\mathbf{y}) \mathbf{M} \mathbf{m}$ is the derived measurement. A candidate UIO for partial-state and message estimations is given by

$$\begin{cases} \dot{\mathbf{z}} = \begin{bmatrix} \mathbf{f}_2(\mathbf{y}, \hat{\mathbf{x}}_2, \hat{\mathbf{m}}) \\ \mathbf{A}_m \hat{\mathbf{m}} \end{bmatrix} + \begin{bmatrix} \mathbf{B}_{2m}(\mathbf{y}, \hat{\mathbf{x}}_2) \mathbf{M} \hat{\mathbf{m}} \\ \mathbf{0} \end{bmatrix} - \begin{bmatrix} \mathbf{L}_{1o}(\mathbf{x}_1) \\ \mathbf{L}_{2o}(\mathbf{x}_1) \end{bmatrix} [\mathbf{f}_1(\mathbf{y}) + \mathbf{B}_{1m}(\mathbf{y}) \mathbf{M} \hat{\mathbf{m}}], \\ \hat{\mathbf{w}} = \mathbf{z} + \mathbf{p}(\mathbf{x}_1), \\ \mathbf{y} = \mathbf{x}_1. \end{cases} \quad (61)$$

If the gains $\mathbf{L}_{1o}(\mathbf{x}_1)$ and $\mathbf{L}_{2o}(\mathbf{x}_1)$ exist such that (61) is asymptotically stable, then $\hat{\mathbf{x}}_2(t) \rightarrow \mathbf{x}_2(t)$ and $\hat{\mathbf{m}}(t) \rightarrow \mathbf{m}(t)$ as $t \rightarrow \infty$. ■

Example 3: Chua's circuit [50]

Consider the Chua circuit described by (8), modified here with an additive message m as,

$$\begin{cases} \dot{\mathbf{x}} = \begin{bmatrix} \alpha(x_2 - x_1^3 - cx_1) + m \\ x_1 - x_2 + x_3 \\ -\beta x_2 \end{bmatrix} = \mathbf{f}(\mathbf{x}) + \begin{bmatrix} 1 \\ 0 \\ 0 \end{bmatrix} m \triangleq \mathbf{f}(\mathbf{x}) + \mathbf{B}_m(\mathbf{x})m, \\ \dot{m} = A_m m, \end{cases} \quad (62)$$

where $\alpha = 10$, $\beta = 16$ and $c = -0.14$ are the chaotic parameters [50]. A different modification scheme is given in Ref. [51].

Using (52), let the output be chosen as

$$\mathbf{y} = \begin{bmatrix} y_1 \\ y_2 \end{bmatrix} = \begin{bmatrix} x_1 \\ x_2 \end{bmatrix} \triangleq \mathbf{x}_1 \Rightarrow \mathbf{w} = \begin{bmatrix} x_3 \\ m \end{bmatrix}, \quad (63)$$

where x_3 constitutes the unknown partial state, and the derived measurement can be obtained as

$$\mathbf{y}_d = \underbrace{\begin{bmatrix} \dot{y}_1 \\ \dot{y}_2 \end{bmatrix}}_{\dot{\mathbf{y}}} - \underbrace{\begin{bmatrix} \alpha(x_2 - x_1^3 - cx_1) \\ x_1 - x_2 \end{bmatrix}}_{\mathbf{f}_w(y_1, y_2)} = \underbrace{\begin{bmatrix} 0 & 1 \\ 1 & 0 \end{bmatrix}}_{\mathbf{B}_w} \underbrace{\begin{bmatrix} x_3 \\ m \end{bmatrix}}_{\mathbf{w}}. \quad (64)$$

Using (62) and (63), the combined partial-state and message system has the form

$$\dot{\mathbf{w}} = \mathbf{A}_w \mathbf{w} + \mathbf{g}(y_2), \quad (65)$$

where $\mathbf{A}_w = \mathbf{0}$ if $A_m = 0$, $\mathbf{g}(y_2) = [-\beta x_2 \quad 0]^T$, and $[\mathbf{A}_w, \mathbf{B}_w]$ is an observable pair for all \mathbf{A}_w , i.e., $\text{rank}[\mathbf{B}_w^T \quad \mathbf{A}_w^T \mathbf{B}_w^T] = 2$.

Using (61) or (65) and (62), a UIO for partial-state and message estimations can be constructed based on \mathbf{y}_d given by (64) and implemented as

$$\begin{cases} \dot{\mathbf{x}} = \mathbf{f}(\mathbf{x}) + \mathbf{B}_m(\mathbf{x})m, & \mathbf{x}(0) = \mathbf{x}_o, \\ \dot{\mathbf{z}} = (\mathbf{A}_w - \mathbf{L}_o \mathbf{B}_w)\mathbf{z} + \mathbf{g}(y_2) + [(\mathbf{A}_w - \mathbf{L}_o \mathbf{B}_w)\mathbf{L}_o \mathbf{y} - \mathbf{L}_o \mathbf{f}_w(y_1, y_2)], & \mathbf{z}(0) = \mathbf{z}_o, \\ \hat{\mathbf{w}} = \mathbf{z} + \mathbf{L}_o \mathbf{y}, & (\mathbf{A}_w = \mathbf{0}, \quad \mathbf{p}(\mathbf{x}_1) = \mathbf{L}_o \mathbf{y}, \quad \mathbf{y} = \mathbf{x}_1). \end{cases} \quad (66)$$

The gain \mathbf{L}_o used for the simulations was obtained by choosing the UIO poles as $\mathbf{p}_o = -[1000 \quad 500]$. Using Matlab's pole-placement command $\mathbf{L}_o = \text{place}(\mathbf{A}_w', \mathbf{B}_w', \mathbf{p}_o)'$, we obtain, with $\mathbf{A}_w = \mathbf{0}$,

$\mathbf{L}_o = 0$	1000
500	0

The message $m(t)$ in (66) is a stock price data consisting of 50 data points where the value of $m(0)$ is $m(0) = 37$. To minimize the effect of $m(t)$ on the chaotic nature of the Chua circuit, it is scaled down to a small signal as $\bar{m}(t) = 0.01m(t)$; this yields $\bar{m}(0) = 0.37$. The scaled down signal was then injected into (62) directly. To enhance the estimate $\mathbf{z}(t) = \hat{\mathbf{w}}(t) - \mathbf{L}_o \mathbf{y}(t) = [\hat{x}_3(t) \hat{\bar{m}}(t)]^T - \mathbf{L}_o [x_1(t) \quad x_2(t)]^T$, its initial value $\mathbf{z}(0)$ was calculated by using $\mathbf{z}(0) = [\hat{x}_3(0) \hat{\bar{m}}(0)]^T - \mathbf{L}_o [x_1(0) \quad x_2(0)]^T$, which gave $\mathbf{z}(0) = [498 \quad -999.63]^T$, where $\hat{x}_3(0) = x_3(0) = -2$ and $\hat{\bar{m}}(0) = \bar{m}(0) = 0.37$. We remark that, since the initial condition $\mathbf{x}(0) = [2 \quad -0.5 \quad -2]^T$ of the Chua circuit is known, we can always set $\hat{x}_3(0) = x_3(0)$, while in the event that the value of $\bar{m}(0)$ is not known, then it can be set as $\bar{m}(0) = 0$ resulting in small mismatches between $\hat{\bar{m}}(t)$ and $\bar{m}(t)$ during the transient period. The performance of the reduced-order UIO is shown in **Figures 6** and **7**. **Figure 6(a)** shows $x_3(t)$ and its estimate $\hat{x}_3(t)$, while **Figure 6(c)** shows the plot of $x_3(t)$ vs. $\hat{x}_3(t)$, which indicates an excellent match. **Figure 6(b)** displays the message $m(t)$ and its estimate $\hat{m}(t)$, while the plot of $m(t)$ vs. $\hat{m}(t)$ in **Figure 6(d)** shows a clean 45-degree line indicating an almost perfect match. The plots of $\{x_i(t), \bar{m}(t) \neq 0\}$ vs. $\{x_i(t), \bar{m}(t) = 0\}$ are depicted in **Figure 7(a)–(c)**, showing that the small signal $\bar{m}(t)$ has little effect on the chaotic nature of the Chua circuit. We conclude that the performance of the reduced-order UIO for partial-state and message estimations was satisfactory. Further, it is emphasized that no Jacobian linearization was employed in this example.

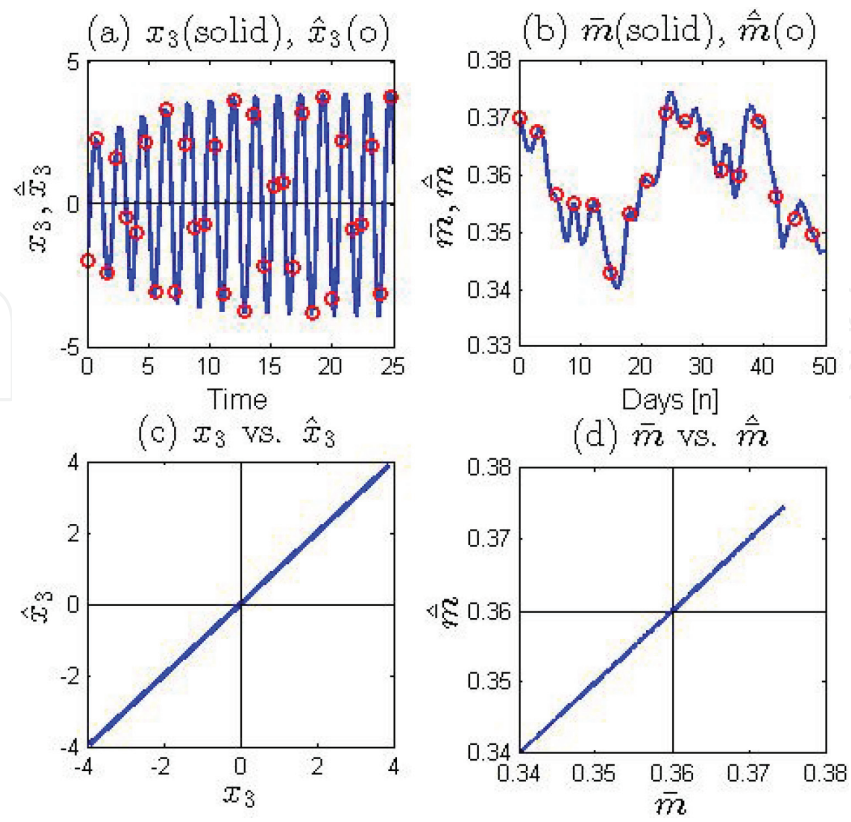


Figure 6. Responses of Chua system: (a) x_3 and \hat{x}_3 ; (b) \bar{m} and $\hat{\bar{m}}$; (c) x_3 vs. \hat{x}_3 ; and (d) \bar{m} vs. $\hat{\bar{m}}$. Figures 6(c) and 6(d) indicate negligible estimation errors $\tilde{x}_2 = x_2 - \hat{x}_2$ and $\tilde{\bar{m}} = \bar{m} - \hat{\bar{m}}$, respectively.

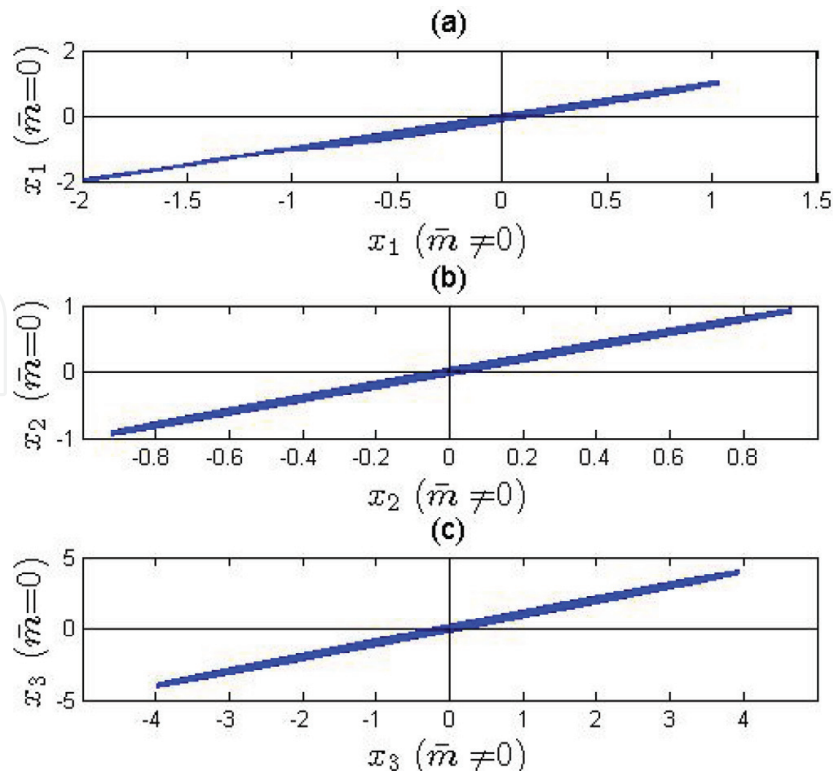


Figure 7. Plots of $x_i (\bar{m} \neq 0)$ vs. $x_i (\bar{m} = 0)$ showing that \bar{m} has little effects on the chaotic nature of the Chua system.

5. Conclusions and plan for future research

In this paper, we showed that secure communication employing chaotic systems can be achieved by synchronizing the dynamics of the drive and response systems. The results are obtained by using unknown-input observers (UIOs), which serve as the response systems. Three classes of UIOs have been designed, namely, (i) full-order UIO for estimating all the state variables (full state) and messages in the drive system; (ii) reduced-order UIO for message estimation based on a derived measurement technique, where the formulation is based on the disturbance observer-based control (DOBC) theory (recall that the DOBC technique is only applicable to disturbance estimation based on the assumption that all the state variables (full state) in a system are known; and (iii) reduced-order UIO for partial-state and message estimations based on partial-state measurement using the derived-measurement technique. The reduced-order UIO for partial-state and message estimations is novel, and is an extension of the DOBC theory, thereby expanding the technique and applications of DOBC. Our future research and development will be focused on wireless secure communication, robust synchronization in the presence of channel noise and various channel induced distortions, and the designs and applications of disturbance cancellation nonlinear control systems using the well-known disturbance accommodation control (DAC) theory, thereby unifying the DAC and DOBC approaches and techniques.

Author details

Robert N.K. Loh* and Manohar K. Das

*Address all correspondence to: loh@oakland.edu or das@oakland.edu

School of Engineering and Computer Science, Oakland University, Rochester, Michigan, USA

References

- [1] Rehan K, Qiao G. A survey of underwater acoustic communication and networking techniques. *Research Journal of Applied Sciences, Engineering and Technology*. 2013;5: 778–789
- [2] Haug OT. Acoustic communication for use in underwater sensor networks [thesis]. Norwegian University of Science and Technology; 2009
- [3] Zielinski A. Communications underwater, Invited presentation. *Journal of Hydroacoustics*. 2004;7:235–252
- [4] Stojanovic M. Underwater acoustic communication. In: *Wiley Encyclopedia of Electrical and Electronics Engineering*. Hoboken, New Jersey, USA: Wiley Interscience; 1999
- [5] Akyildiz IF, et al. Challenges for efficient communication in underwater acoustic sensor networks. *CM SIGBED Review. Embedded Sensor Networks and Wireless Computing*. 2004;1(Special issue):3–8

- [6] Melodia T, et al. Advances in underwater acoustic networking. In: *Mobile Ad Hoc Networking: Cutting Edge Directions*. 2nd ed. Wiley Online Library. Chapter 23; 2013
- [7] Yue J-P, et al. A robust wide synchronous digital chaotic communication scheme in shallow water channel. In: *Proceedings of the Fourth International Workshop on Chaos-Fractals Theories and Applications (IWCFTA)*. 19–22 October 2011. New York: IEEE; 2011. pp. 203–207
- [8] Shu X, et al. Chaotic modulations and performance analysis for digital underwater acoustic communications. *Applied Acoustics*. 2016;**105**:200–208
- [9] Shu X, et al. Chaotic direct sequence spread spectrum for secure underwater acoustic communication. *Applied Acoustics*. 2016;**104**:57–66
- [10] Ren H-P, et al. A chaotic spread spectrum system for underwater acoustic communication. *Physica A: Statistical Mechanics and its Applications*. 2017;**478**:77–92
- [11] Shu X, et al. Underwater chaos-based DS-CDMA system. In: *Proceedings of IEEE International Conference on Signal Processing Communications and Computing*. 19–22 Sept. 2015. New York: IEEE; 2015
- [12] Azou S, Burel G, Pistre C. A chaotic direct-sequence spread-spectrum system for underwater communication. In: *Proceedings of IEEE Oceans*. 29–31 Oct. 2002. New York: IEEE; 2002. pp. 2409–2415
- [13] Ren H-P, et al. Experimental validation of wireless communication with chaos. *Chaos*. 2016;**26**:083117
- [14] Ren H-P, et al. Wireless communication with chaos. *Physics Review Letters*. 2013;**110**:184101
- [15] Yao J-L, et al. Chaos-based wireless communication resisting multipath effects. *arXiv*: 1611.02325 [cs.IT]
- [16] Kaddoum G. Wireless chaos-based communication systems: A comprehensive survey. *IEEE Access*. 2016;**4**:2621–2648
- [17] Al-Hussaibi, Walid A. Effect of filtering on the synchronization and performance of chaos-based secure communication over Rayleigh fading channel. *Communications in Nonlinear Science and Numerical Simulation*. 2015;**26**:87–97
- [18] Al-Hussaibi, Walid A, et al. On the synchronization of secure wireless communication systems based on chaotic circuits. *Open Transactions on Wireless Communications*. In Press. Available from: www.scipublish.com/journals/WSN/papers/download/3306-1428.pdf [Accessed: 15-06-2017].
- [19] Jiancheng Z, Fanglai Z. Chaos synchronization and chaos-based secure communication based on new unknown input observer approach. In: *Proceedings of the 35th Chinese Control Conference*. 27–29 July 2016. New York: IEEE; 2016. pp. 1891–1896

- [20] Yang J, Zhu F. Synchronization for chaotic systems and chaos-based secure communications via both reduced-order and step-by-step sliding mode observers. *Communications in Nonlinear Science and Numerical Simulation*. 2013;**18**:926–937
- [21] Yang J, Chen Y, Zhu F. Associated observer-based synchronization for uncertain chaotic systems subject to channel noise and chaos-based secure communication. *Neurocomputing Archive*. 2015;**167**:587–595
- [22] Yang J, Zhu F. Synchronization for chaos-based secure communications via reduced-order and step-by-step sliding mode observers. *Communications in Nonlinear Science and Numerical Simulation*. 2013;**18**:926–937
- [23] Chang W-D, Shih S-P, Chen C-Y. Chaotic secure communication systems with an adaptive state observer, *Journal of Control Science and Engineering*. 2015;**2015**:1–7. Available from: <http://dx.doi.org/10.1155/2015/471913> [Accessed: 28-03-2017]
- [24] Johnson CD. Accommodation of disturbances in linear regulators and servomechanism problems. *IEEE Transactions on Automatic Control*. 1971;**AC-16**:635–644
- [25] Johnson CD. On observers with unknown and inaccessible inputs. *International Journal of Control*. 1975;**21**:825–831
- [26] Johnson CD. Theory of disturbance-accommodating controllers. In: *Control and Dynamic Systems, Advances in Theory and Applications*. In: Leondes CT, editor. Cambridge, MA, USA: Academic Press; 1976. pp. 387–489
- [27] Ciccarella G, Dalla Mora M, Germani A. A Luenberger-like observer for nonlinear systems. *International Journal of Control*. 1993;**57**:537–556
- [28] Mora MD, Germani A, Manes C. A state observer for nonlinear dynamical systems. *Nonlinear Analysis, Theory, Methods, & Applications*. 1997;**30**:4485–4496
- [29] Friedland B. *Advanced Control System Design*. New Jersey, USA: Prentice-Hall; 1996
- [30] Glad T, Ljung L. *Control Theory, Multivariable and Nonlinear Methods*. Abingdon, Oxfordshire, UK: Taylor and Francis. 2000
- [31] Besancon G. An Overview on Observer Tools for Nonlinear Systems. In: *Nonlinear Observers and Applications*. Berlin, Germany: Springer-Verlag. 2007
- [32] Kravaris C, Sotiropoulos V, Georgiou C, Kazantzis N, Xiao MQ, and Krener AJ. Nonlinear observer design for state and disturbance estimation. *Systems & Control Letters*. 2007;**56**:730–735
- [33] Sundarapandian V. Reduced-order observer design for nonlinear systems. *Applied Mathematics Letters*.; 2006;**19**:936–941
- [34] Trinh H, Fernando T. *Functional Observers for Dynamical Systems*. Berlin, Germany: Springer-Verlag. 2011. p. 227

- [35] Pecora LM, Carroll T. Synchronization in chaotic systems. *Physical Review Letters*. 1990;**64**:821–824
- [36] Inoue E, Ushio T. Chaos communication using unknown input observers. *Electronics and Communication in Japan*. 2001;**84**(12):21–27
- [37] Feki M. An adaptive chaos synchronization scheme applied to secure communication. *Chaos, Solitons and Fractals*. 2003;**18**:141–148
- [38] Chen M, Zhou DG, Shang Y. A new-observer-based synchronization scheme for private communication. *Chaos, Solitons and Fractals*. 2005;**24**:1025–1030
- [39] Chen M, Wang M. Unknown input observer based chaotic secure communication. *Physics Letters A*. 2008;**372**:1595–1600
- [40] Wang XY, Wang MJ. A chaotic communication scheme based on observer. *Communication in Nonlinear Science and Numerical Simulation*. 2009;**14**:1502–1508
- [41] Grzybowski JMV, Eisencraft M, Macau EEN. Chaos-based communication systems: Current trends and challenges. In: Banerjee S, et al., editors. *Application and Nonlinear Dynamics in Engineering; 1: Understanding Complex Systems*. Heidelberg: Springer-Verlag; 2011. Chapter 7
- [42] Mata-Machuca JL, Martinez-Guerra R, Aguilar-Lopez R. A chaotic system in synchronization and secure communications. *Communications in Nonlinear Science and Numerical Simulation*. 2012;**17**:1706–1713
- [43] Yau HT, Pu YC, Li S. Application of a chaotic synchronization system to secure communication. *Information Technology and Control*. 2012;**41**:274–282
- [44] Dimassi H, Loria A, Belghth S. A new secured transmission scheme based on chaotic synchronization via smooth adaptive unknown input observers. *Communications in Nonlinear Science and Numerical Simulation*. 2012;**17**:3727–3739
- [45] Wang XY, Wang MJ. A chaotic secure communication scheme based on observer. *Communications in Nonlinear Science and Numerical Simulations*. 2009;**14**:1502–1508
- [46] Mata-Machuca J, Martinez-Guerra R, Aguilar-Lopez R. A chaotic system in synchronization and secure communications. *Communications in Nonlinear Science and Numerical Simulation*. 2012;**17**:1706–1713
- [47] Rossler OE. An equation for continuous chaos. *Physics Letters A*. 1976;**57**:397–398
- [48] Strogatz ST. *Nonlinear Dynamics and Chaos with Applications to Physics, Biology, Chemistry, and Engineering*. 2nd ed. Boulder: Westview Press; 2015
- [49] Genesio R, Tesi A. A harmonic balance methods for the analysis of chaotic dynamics in nonlinear systems. *Automatica*. 1992;**28**:531–548
- [50] Chua L, Komuro M, Matsumoto T. The double scroll family. *IEEE Transactions on Circuits and Systems*. 1986;**33**:1072–1178

- [51] Mauricio Zapateiro De la Hoz M, Acho L, Vidal Y. A secure communication system based on a modified chaotic Chua oscillator. In: Proceedings of 7th CHAOS Conference. 7–10 June 2014; Lisbon. Oakland: ISAST. pp. 563–572
- [52] Moreno J. Unknown input observers for SISO nonlinear systems. In: Proceedings of 39th IEEE CDC Conference. 12–15 December 2000; Sydney. New York: IEEE; 2000. pp. 790–795
- [53] Isidori A. Nonlinear Control Systems. Springer; 1995: p. 549
- [54] Slotine JJ, Li WP. Applied Nonlinear Control. New Jersey: Prentice Hall; 1991: p. 459
- [55] Kalman RE, Bucy RS. New results in linear filtering and prediction theory. ASME Journal of Basic Engineering. 1961;**83**:95–107
- [56] Gelb A. Applied Optimal Estimation. Massachusetts: MIT Press; 1974: p. 374
- [57] Luenberger DG. An introduction to observers. IEEE Transactions on Automatic Control. 1971;**AC-16**:596–602
- [58] Gopinath B. On the control of linear multiple input-output systems. American telephone and telegraph company – The Bell System Technical Journal. 1971;**50**:1063–1081
- [59] Chen CT. Linear System Theory and Design. 4th ed. New York: Oxford University Press; 2013: p. 400
- [60] Ogata K. Modern Control Theory. 5th ed. New Jersey: Prentice Hall; 2010: p. 894
- [61] Li S, Jun Y, Chen W-H, Chen X. Disturbance observer-based control. Methods and Applications. Boca Raton: CRC Press; 2014: p. 342

